MESOSCALE EDDIES AND PLASTIC DISPERSION

T H E S I S

Master of Science,
Climate Physics

MARIANA DE BOTTON FALCÓN

Supervisors:
PROF DR. ERIK VAN SEBILLE
DR. LAURA GÓMEZ NAVARRO

December 2021

OceanParcels

Acknowledgements

Abstract

It is widely accepted that floating plastic debris have a negative effect on the ocean environment. However, while the variability in plastic concentrations in the ocean is well understood on the gyre scale (Ekman dynamics), little is known about the variability on the mesoscale. For these reasons, it is important to gain a better understanding of the distribution of plastic in the ocean. Thus, the objectives of this work include exploring the possible relationship between the concentration of surface microplastic within mesoscale eddies and the flow direction of the eddies, the potential relationship of chlorophyll and eddy activity, as well as the ways in which mesoscale eddy dynamics may influence the transport of surface microplastic. To achieve this, plastic data from surface trawling nets was collected from multiple sources, and analyzed for the time period 1995-2019. The analysis was carried out with respect to eddy mechanisms in the ocean, with eddies identified by an eddy-tracking tool, using sea level anomaly data as the input. The relation to remote sensed chlorophyll-a concentration data at the surface of the ocean was also studied in the main areas of interest – the North Atlantic, the North Pacific and Worldwide. Anticyclonic eddies were observed to contain higher percentage of plastic concentrations in all areas of interest compared to cyclonic eddies. Except for the North Atlantic region, the highest percentage of plastic was found outside of eddies. Data in other regions was too sparse to support making similar conclusions, as more data will be necessary to fill in the gaps and being able to investigate on a global scale the relationship between plastic marine debris and eddy dynamics.

Contents

List of Figures

Introduction

1.1.   State of the art

It is known that plastic debris affects the ocean environment and it is a systemic problem that we are dealing with on a global scale. Being able to evaluate the levels of plastic pollution and its dynamics will lead to knowledge about plastic accumulation and distribution and its relationship with eddies, which could be useful as a proxy for oceanic plastic distribution modelling, as well as in helping us to correctly asses the severity of the damage that plastic does to the marine environment (Everaert et al. [11]). There are a number of different methodologies used for the sampling of this type of plastic, and thus comparing the different data-sets of floating plastic debris is difficult as it is not uniform. With this in mind, the primary data-set used for purposes of analysis in this thesis is the one from van Sebille et al. 2015 [37], and which is composed of a collection of measurements of small plastic debris (< 200 mm) at the surface of the ocean sampled with surface-trawling plankton nets.

Due to the large-scale ocean dynamics, marine plastic at the surface of the ocean has been found to accumulate at the ocean gyres (Law et al. 2010 [24], Eriksen et al. 2013 [10]). This is described by geostrophy theory in large-scale circulation, which quite successfully predicts the distribution of floating microplastic on a large scale (van Sebille et al. 2020 [38]). The complex dynamics of the ocean make it so that the plastic distribution and amount of plastic present at the ocean surface is difficult to track and predict, as many elements of these dynamics play a role in the dispersion and distribution of floating debris (e.g. Stokes drift, internal tides, wind transport etc.). One possibly important aspect of these dynamics for the distribution of plastic are mesoscale eddies, which are ocean phenomenon that can be characterized as

vortices or similar structures, on scales of hundreds of kilometeres, and with lifetimes anywhere from weeks to years (van Sebille et al. 2020 [38]). Eddies can transport fluid parcels within themselves (Chelton et al. 2011 [4]), and could thus give us a clearer picture of the distribution and transport of plastic particles in the ocean.

There are two types of eddies, anticyclonic and cyclonic. Anticyclonic eddies flow clockwise in the Northern Hemisphere and form a positive sea level anomaly within themselves (as there is downwelling at the center (Chelton et al. 2007 [5])). On the other hand, cyclonic eddies flow counter-clockwise in the Northern Hemisphere, form a negative sea level anomaly and there is upwelling at their center. These dynamics lead to material suspended in the ocean drifting towards anticyclonic eddies and being expelled from cyclonic ones; however, the complete dynamics of these exchanges are more complex than that (Brach et al. 2018 [2]). In the work of Brach et al. 2018 [2], it was shown that even on a small sample set of eddies, anticyclonic eddies have up to 9.4 times the concentration of plastic within them than cyclonic eddies do, impacting the distribution of plastic in subtropical gyres as well as the dynamics of the distribution of the plastic. Eddies also transport other matter apart from plastics (like plankton), nonetheless this form of transport was left as an open research question by Brach et al. 2018 [2] – to determine the relationship between plankton and eddy plastic accumulation, as well as to determine the movement of plastic within the eddies' surface, taking into account the leakage of material from the eddies as well as their non-uniform boundaries. It is important to note that the Brach et al. 2018 [2] study was performed on a small portion of the North Atlantic, specifically between 15 and 30°N and 55 and 65°W from the 28th May to the 16th June 2015. To our knowledge Brach et al. 2018 [2] is the only study which has looked into the impact of eddies on the dispersion of marine plastic.

1.2. Motivation

As we mentioned before, the presence of plastic in the ocean pollutes the marine environment, and for this reason we need to develop a better understanding since it poses a significant risk to wildlife. As per Everaert et al. [11], a staggering median level of 1.21×10^5 microplastic counts per meter cubed was calculated to be present in the global ocean. Furthermore, this study concluded that in 2010, for 0.17% of the surface layer between 0 and 5 meters

of the global ocean, a threatening risk for wildlife is present. This fraction is only expected to increase, and by 2050 Everaert et al. predict this area to grow to 0.52% of the surface ocean, with hotspots in the Mediterranean and Yellow seas respectively. This poses a clear danger for future generations, and it is thus highly valuable for us to work on improving our understanding, to be able to find better ways to combat the issue of plastic pollution in the oceans.

In Section 1.1, it was noted that Brach et al. [2] left as future work to investigate the possible differences in plastic concentration in cyclonic/anticyclonic eddies in other parts of the global ocean, as their study covered only a small portion of the North Atlantic. As part of this thesis, we intend to do exactly that, by leveraging the data-set assembled by van Sebille et al. [37]. To make the overall analysis more comprehensive, further additional data-sets were incorporated, from studies conducted after 2014.

An interesting known phenomena is that cyclonic eddies generally have a larger concentration of plankton within them, as due to upwelling more nutrients flow from deeper ocean layers, facilitating plankton growth (He et al. 2017 [15]). Thus, while we are investigating the concentration of plastic, it is also interesting for us to explore what happens to the plankton at the surface of the ocean in locations of surface plastic within eddies, in a general way, using plankton growth as a proxy for biodiversity (Sherman and van Sebille 2016 [40]).

Finally, this leaves us with the research questions for this work:

1. In regions other than the small section of the North Atlantic explored by Brach et al. [2], where mesoscale eddies are present, is there a correlation between the concentration of microplastic within eddies at the surface and the flow direction of the eddies?

2. How does the dynamic of mesoscale eddies influence the transport of microplastic at the surface?

3. What, if any, relationship of biodiversity (chlorophyll) and plastic can be observed, with regard to eddy activity – where eddy activity is characterized by sea level anomaly, plastic observations within eddies, as well as the eddy flow direction?

Theoretical background

2.1. Small plastic debris

Plastic found in the world oceans is highly widespread. This is widely believed to be caused by the fact that these plastics break down at a very slow rate, and mostly by virtue of UV exposure and physical damage/abrasion. Additionally, most of such plastic is highly buoyant, with roughly two thirds being lighter than sea water, and other forms having air trapped within the structure. These factors together make it so plastic moves within the oceans with ease with the aid of wind, and a large quantity stays at the ocean surface (van Sebille et al. 2020 [38]).

During the process of breaking down, the plastic pieces found in the ocean can become very small – even <5mm in diameter, at which point the resulting pieces are conventionally referred to as microplastic. However, in this work, we will be adopting the small plastic debris definition for microplastic as per van Sebille et al. 2015 [37], where any plastic debris smaller than 200 mm in diameter are regarded as microplastic. Such floating plastic debris are then transported across the large bodies of water by means of Stokes drift, internal tides, windage, Langmuir circulation, large scale ocean circulation among other ways.

A particle floating on the free surface of a surface gravity wave experiences a net drift velocity in the direction of wave propagation, and this phenomenon is known as the Stokes drift (Stokes 1847 [42]). In other terms, the Stokes drift velocity is the difference between the average Lagrangian flow velocity of a fluid parcel and the average Eulerian flow fluid velocity (van Sebille et al. 2020 [38]). It is still an open research question whether floating plastic debris

are in fact consistently transported with the velocity of their surrounding Lagrangian flow and with it, with Stokes drift.

The effect of wind on items with an area protruding out of the water (freeboard) is called windage. This wind induced displacement can be directly related to the wind speed (Tapia et al 2004 [44]), however it is important to note that windage does not correspond to the part of the surface flow field driven by the wind (and which is already part of the surface current), but to the direct wind drag on sea surface items (Zambianchi et al 2014 [46]). Thus, the effect of windage is in practice typically combined with the Stokes drift, into the so called 'leeway' – defined as the wind and wave induced motion on a drifting object, relative to the ambient current (Breivik et al 2013 [3]).

The movement of tides over reefs, banks and the continental shelf break produces large internal waves generated by internal tides (Kao et al. 1985 [22]). These internal waves are most commonly generated at the continental shelf break. A lee wave (hydraulic jump) is produced over the continental slope as the tide ebbs off the shelf. As the tide changes to flood, the lee wave propagates shoreward and on the shelf, where it turns into a train of internal waves. As these waves move into shallower water, they can break, forming an internal bore (Pieneda et al 1995 [33]). Surface currents are then generated over the internal waves, and at the surface over the leading edge of the wave such currents turn downward forming a surface convergence – which moves along with the wave. In the case of waves of depression, the surface current is in the direction of the propagation of the wave, and in case of larger depression waves, the surface current can be sufficiently fast to carry objects at the surface (such as plastic debris and flotsam) to the convergence (Shanks et al 2000 [39]).

In certain cases, the surface flow can form coherent roll structures – pairs of counter-rotating vortices aligned horizontally. One of the best known flows of this type is Langmuir circulation (Langmuir 1938 [18]), for which windrows are formed. Windrows are lines of bubbles and surface debris generally aligned with wind, and they represent the convergence zones between helical vortex pairs of Langmuir circulation. These circulation cells are often areas of accumulation for planktonic organisms and floating plastic debris, potentially enhancing biofouling as well as plastic consumption by biota (Gove e al. 2019 [14]).

In the case of large scale ocean circulation, one of the main drivers are surface winds (van Sebille et al. 2020 [38]). Here the winds together with the rotation of the Earth generate an Ekman drift perpendicular and to the right

of the wind in the northern hemisphere and to the left in the southern hemisphere. The resulting Ekman transport, produces regions where the surface converges and diverges, and these motions drive the geostrophic flow of the ocean interior on a large scale. Convergence of the surface flow can then be observed in all five subtropical gyres, while surface flow divergence is found in subpolar gyres and in parts of the Southern ocean. Thus, a notable amount of plastic is moved by these dynamics, and ends up accumulating in converging surface areas, while at the same time, lower quantities of plastic are found in areas of divergence. In the case of smaller scale convergence regions, Ekman downwelling occurs, where surface water is propelled down, to below the depths of 100 m. However, the velocity of the donwelling is far lower at the surface, meaning that it is not sufficient to transport floating debris with it, leaving them behind at the surface (Poulain et al. 2019 [34]).

The theory of large scale circulation and geostrophy described above, quite successfully predicts the distribution of floating microplastic on a large scale (van Sebille et al. 2020 [38]), with one of the notable products of the model of large scale circulation being the collecting of plastic in the "garbage patches" within the subtropical gyres. These patches also change over time, and are heterogeneous with plastic debris, with a few important exceptions – the main one being the North Pacific accumulation zone (van Sebille et al. 2015 [37]).

2.2. Mesoscale eddies

Mesoscale eddies are vortices with a slow directed rotation, and diameter of hundreds of kilometeres, and depths of a couple hundred to possibly thousands of meters, and lifetime anywhere from weeks to years (van Sebille et al. 2020 [38], Chelton et al. 2011 [4], Mason et al. 2014 [29]). Mesoscale eddies are quite ubiquitous in the ocean, and are capable of transporting properties such as heat, carbon and slat around the ocean. By straining the surface waters, these eddies may also form filaments and fronts, which become unstable and then form submesoscale eddies (smaller, faster changing eddies on the 1-10 km scale, and with a lifetime of days to weeks, van Sebille et al. 2020 [38]). Furthermore, mesoscale eddies exist in two types, as visualised in Figure 2.1:

- Cyclonic eddies – These eddies rotate counter-clockwise in the northern hemisphere, and clockwise in the southern, with surface flow primarily outward

- Anticyclonic eddies – These eddies rotate clockwise in the northern hemisphere, and counter-clockwise in the southern, with surface flow primarily inward
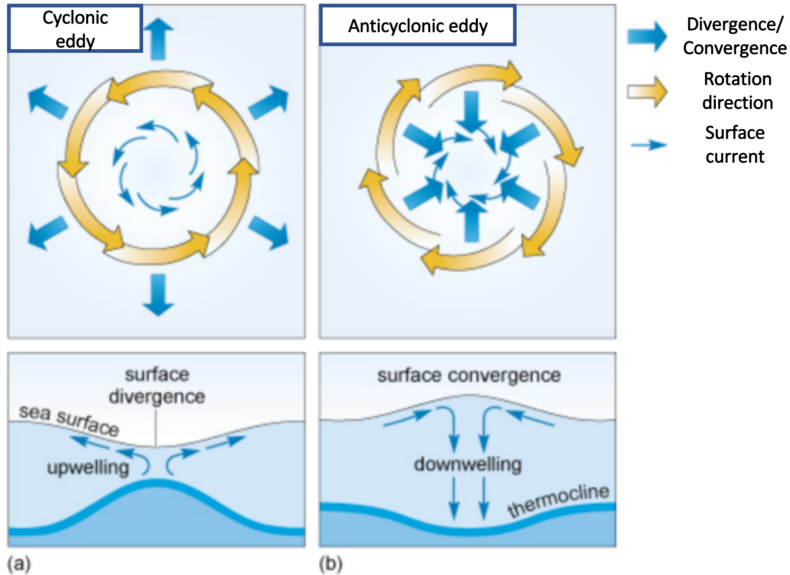
Figure 2.1: Cyclonic and Anticyclonic eddy dynamics illustrated (modified from Open Learn Ocean Currents, Chapter 4.4 [31])

The anticyclonic eddies are in this way similar to gyres in that they flow inward, and so produce an area of convergence (while the opposite is true for cyclonic) – which can aid in explaining the observation that more floating debris were found in an anticyclonic eddy rather than in a cyclonic one (Brach et al 2018 [2]). It is worth noting that submesoscale eddies are more effective at accumulating debris (van Sebille et al. 2020 [38]), however the eddies with the longest lifetimes and propagation distances are predominantly mesoscale anticyclonic eddies (Fu et al. 2010 [25]).

Onken et al 2021 [30] modelled an cyclonic spiral of 1km in diameter with ROMS (Regional Ocean Modeling System), using 33.3m horizontal resolution in a triple-nested configuration. The generation of this spiral starts from a dense filament, which is rolled into a vortex and then detaches from the filament. During the resulting spin-down after detaching, the horizontal speed develops a dipole-like pattern and isotachs form closed contours around the vortex center. Downwelling is indicated everywhere near the surface, while it

is strongest in the center of the spiral at all depths, leading to a radial outflow in the thermocline and weak upwelling at the periphery – this overturning circulation is driven by convergent near-surface flow and associated subduction of isopycnals. The downwelling at the center thus may support the export of organic carbon particles from the mixed layer into the main thermocline, however, the upwelling at the periphery supports an upward isopychnal transport of nutrients, boosting plankton growth in the euphotic zone (Onken et al 2021 [30]).

A phenomenon called eddy pumping is used to define the upwelling and downwelling produced during eddy intensification. When anticyclonic (cyclonic) eddies intensify, isopycnals are depressed (uplifted) creating downwelling (upwelling) at the eddy center, with associated vertical velocities of up to $1m/d$ (Gaube et al. 2014 [13]). This may lead to increased chlorophyll at the surface of cyclonic eddies, and reduction and downward transport of chlorophyll in anticyclonic eddies (Hernández-Hernández 2020 [16]). With this in mind, it is then interesting to note that high concentrations of chlorophyll were often observed at the core of cyclonic eddies, and the opposite was true for anticyclonic ones (Kouketsu et al. 2016 [23]). This can be attributed to the upwelling caused by cyclonic eddies, where the isotherms are domed upwards, which may bring up new nutrients from lower layers of the ocean into the euphotic zone, thus allowing algal cells to flourish in the core of the eddy (Leterme et al. 2008 [26]) – meaning that coldcore rings are thus generally higher in Chl-a. Such relationships between chlorophyll concentrations and eddies were not commonly observed in the southern part of the North Pacific recirculation gyre (142°E–152°E and 28.5°N–31.5°N), where southward (northward) advection of water with high (low) Chl-a concentrations around the eddies accounted for most of the Chl-a concentration patterns both for anticyclonic and cyclonic eddies (Kouketsu et al. 2016 [23]).

The convergence and divergence properties of eddies imply that retention times of plankton in cyclonic eddies should increase with increasing depth (and vice versa for anticyclonic eddies). These properties further imply that slowly sinking plankton (e.g. diatoms) is more likely to be found in cyclonic eddies, while anticyclonic eddies are likely to favour upwardly motile plankton (e.g. dinoflagellates). The reason this distinction is important is because diatoms typically support food webs with higher trophic levels dominated by finfish, while dinoflagellates support more gelatinous organisms (Condie et al. 2016 [8]).

Mesoscale eddies owe their stability to the geostrophic balance, in which gravitational forces are compensated by Coriolis forces (Williams 2011 [45]). In terms of their formation, the largest scale eddies emerge from barotropic instabilities associated with strongly horizontally sheared motions, especially in the case of the boundary currents (and their extensions into the ocean interior) such as the Gulf Stream, where eddies often extend to large depths, form well defined rings, and their mean amplitudes can exceed 30cm (Fu et al. 2010 [25]). Furthermore, the eddies produced by the Gulf Stream have a roughly equal distribution between being produced as cyclonic and as anticyclonic eddies (Kang et al. 2013 [20]). In the case of smaller mesoscale eddies (tens of km), they are produced by baroclinic instability of the mean currents, and this primarily happens in strongly stratified fluids where there is a vertical shear of the horizontal velocity – in which case the fluid can be in geostrophic equitibrium but not at the lowest energy level possible, so there is a supply of available potential energy (Williams 2011 [45]). Both of these processes of eddy creation have hot spots of production in the vicinity of western boundary currents and the Antarctic Circumpolar Current. In the eastern boundary current regions such as with the California Current, the mean eddy amplitudes are moderately large and the formation is frequent (Chelton et al. 2011 [4]), however, the mean amplitudes are only a few centimeters in the ocean interiors away from these regions of high mesoscale variability (Fu et al. 2010 [25]). One other interesting location where eddies are frequently formed is along the various seamountchains northwest of Hawaii. This could be attributed to a rapid amplification of the westward propagating eddies, which are too small to be detected by altimetry while they are in the eastern part of the basin, and can only be tracked once their amplitudes grow after encountering these bathymetric features (Chelton et al. 2011 [4]). Alternatively, this could indicate an interaction between the bottom topography and the flow field (including Rossby waves from the eastern basin).

With this in mind, water motions associated with eddies are related to differences in the sea surface height (SSH) from the geoid. For this reason, satellite radar altimetry is very effective for studying eddy dynamics globally. Thus, using sea level anomaly (the difference between the total sea-level and the average annual sea-level), eddies can be detected utilising the following facts (Faghmous et al. 2015 [12]):

- Cyclonic eddies cause a decrease in sea level anomaly (SLA) and upwelling

- Anticyclonic eddies, cause an increase in SLA and downwelling

Therefore, anticyclonic eddies manifest as closed-contours of positive SLA, while cyclonic eddies form closed-contours of negative SLA, which are algorithmically detectable. Applying these principles to eddy detection, in the work of Chelton et al. 2011 [4] a slight preference to cyclonic eddies is noted globally, but anticyclonic are more dominant in the northern hemisphere (Chelton et al. 2011 [4]).

2.3. Biofouling and chlorophyll

Biofouling is the attachment and accumulation of biological organisms on the surface of a submerged object (Lobelle et al. 2021 [27]). The presence of microplastic in the ocean makes it a perfect substrate for microbes to attach to and flourish. The effect of this attachment is the increase in size of the microplastic, thus reducing available light to the lower layers of the ocean, as well as further increasing the thickness of the barrier at the air-sea interface. This also weights down the plastic over time causing it to sink, and take all of the organic carbon with itself to the lower layer, possibly affecting the ocean's carbon pumps and transporting the plastic into the water column as well as the bottom of the ocean, where this plastic can be consumed by animals living in the ocean.

In terms of rate of sinking, the larger the particle, the more likely it is to encounter local algal cells, and so its density can increase faster. However, if the object is smaller, the there is more relative surface area, so even a small number of attached algal cells may cause it to sink. With this in mind, in the work by Lobelle et al. 2021 [27], it was concluded that the smallest particles (0.1 μm) start sinking almost immediately globally (within $\approx$ one day), medium particles (1 μm) take only slightly longer, while the largest particles tested (1, 0.1 and 0.01 mm) all take approximately the same larger amount of time globally (35-38 days). This is interesting, as it provides a possible relative indication for the abundance of surface microplastic in areas of high observed chlorophyll concentration, measured with remote sensing.

A finding of interest, pertinent to the relationship between chlorophyll and sea level anomaly (SLA), was concluded in the work by Hou et al. 2016 [17], where they concluded that the interannual variability of chlorophyll was negatively correlated with the sea surface temperature (SST) and sea level anomaly

(SLA), while it was positively correlated with the wind speed. Therefore, in regions of a negative (positive) SLA, which can correspond to a cyclonic (anticyclonic) eddy, a positive (negative) chlorophyll anomaly is expected. Furthermore, a study by Kanhai et al. 2017 [21] concluded that there was no statistically significant correlation between microplastic concentration and chlorophyll in the oceans.

Methods

In this chapter we will discuss how the plastic data-set was constructed, starting with introducing each individual data type included, then explaining the chosen eddy tracker tool, and concluding with the complete specification of the assembly of the data-set.

3.1. Plastic data-sets

The core of the data used was taken from the publication by van Sebille et al. [37], where plastic data collected with surface-trawling plankton nets with mesh ranging from 0.1 to 0.5 mm, was identified in literature and assembled into one cohesive set. Here, the definition of microplastic used was the same one adopted for this work in Section 2.1, and the core data-set contained both counts per area and mass per area measurements (where available), while this work focuses only on the counts per kilometer squared representing plastic concentration. Furthermore, in the original data-set a generalized additive model (GAM) was applied to obtain a standardization of the plastic measurements – however, for the purposes of this analysis, the raw data from the original data-set was utilized. On the other hand, the same standardization was not applied when extending the core data-set here, but rather the same requirements and specification of the measurements were taken into account instead (same definition of microplastic, microplastic concentration units, taking a maximum measurement depth of 1 m and plankton net falling in range of 0.1 to 0.5mm). With this in mind, the core data-set was then augmented with further measurements taken from the following sources:

- The Ocean Cleanup Project (Egger et al. 2021 [9]) – The data collected here was based on 54 Manta trawl samples collected in the eastern North

Pacific Ocean during two expeditions between August 2015 and December 2019. These measurements were performed using a manta net with an aperture of 90 cm × 15 cm (width height) and a square mesh net of 500 μm (333 μm mesh size cod-end).

- Circumpolar survey by Suaria et al. 2020 [43] – Forty neuston samples were collected around the continent of Antarctic between December 2016 and May 2017, as part of the data contribution of this study. These measurements were collected using a 200 μm neuston net, equipped with a 100 by 30 cm rectangular frame opening, towed for 15 min at a speed of 2–2.5 knots.

- Mediterranean Marine Floating Plastic Mass Budget by Kaandorp et al. 2020 [19] – The data collected and provided as part of this study is a larger collection of contemporary data-sets, where plastic samples were reported from manta trawl or neuston net measurements, among other methods. For the purposes of this work, only the trawl data was used – this covered data from: Baini 2018, Collignon 2012, Galgani 2011, van Der Hal 2017, Guven 2017, Ruiz-Orejon 2016, Zeri 2018, Pedrotti 2016 and de Haan 2019 (refer to Kaandorp et al. 2020 [19] for complete sources).

The data collected was assembled into one larger data-set, with each plastic measurement labelled with its respective originating data-set. All of the measurements collected were ones produced with surface-trawling plankton nets, ensuring compatibility between samples. Furthermore, the final data-set covers the year range from 1995 to 2019, instead of from 1970s to 2014 like the core data-set did, as this was the first year when sea level anomaly data becomes available.

3.2. CMEMS products

The chlorophyll and sea level anomaly data was gathered from the Copernicus Marine Environment Monitoring Service (CMEMS). The data was accessed through the use of their online api, the motuclient. The data specification is as follows:

- The chlorophyll dataset – obtained from the OCEANCOLOUR-GLO-CHL-L4-REP-OBSERVATIONS-009-082 CMEMS product [6], using the variable Chlorophyll-a. This product is based on a multi sensors/algorithms

approach, and the specific variable used is "Cloud Free" in that it is based on a space-time interpolation (called L4). The available data from this CMEMS product spans the date range of 1997-09-04 to present, with one measurement grid per day. The spatial resolution of the grid is 4 km by 4 km.

- The sea level anomaly dataset – obtained from the SEALEVEL-GLO-PHY-L4-REP-OBSERVATIONS-008-047-TDS CMEMS product [7]. Here, the sea level anomalies were computed with altimeter satellites, with respect to a twenty-year 2012 mean, where the SLA is estimated by Optimal Interpolation, merging the measurement from the different altimeter missions available. The available data from this CMEMS product spans the date range of 1993-01-01 to present, with one measurement grid per day. Here the data grid resolution is 0.125° by 0.125°.

3.3. Eddy tracker

To be able to detect eddies for each of the dates where plastic measurements were available, the py-eddy-tracker (Mason et al. [29]) software tool was used. In essence, the tracker detects eddies as follows:

- First, the input SLA field is spatially high-pass filtered by removing a smoothed field obtained from a Gaussian filter, with a zonal (meridional) major (minor) radius of 10° 5°

- Contours are then identified in the filtered SLA field within a specified analysis domain. This is done by computing SLA contours at intervals of 1cm for sea level anomaly levels of 100 to 100 cm

- Each of the identified contours is then analyzed to detect if they are cyclonic or anticyclonic. This is done by iterating the SLA levels from 100 (-100) downward (upward) for the case of detecting cyclonic (anticyclonic) contours Closed contours (C_C) at each of these SLA levels are then sequentially identified and analysed. A C_C is then identified as an eddy if it:

  1. Passes a shape test where the error is $\leq 55\%$ (the error here is defined as the ratio between the areal sum of C_C deviations from the contour's fitted circle and the area of that circle)

  2. Contains a pixel count, I, which satisfies $8 \leq I \leq 1000$

3. Contains only pixels with SLA values above (below) the current SLA interval value for anticyclonic (cyclonic) eddies

4. Contains no more than one local SLA minimum (maximum) for an cyclone (anticyclone)

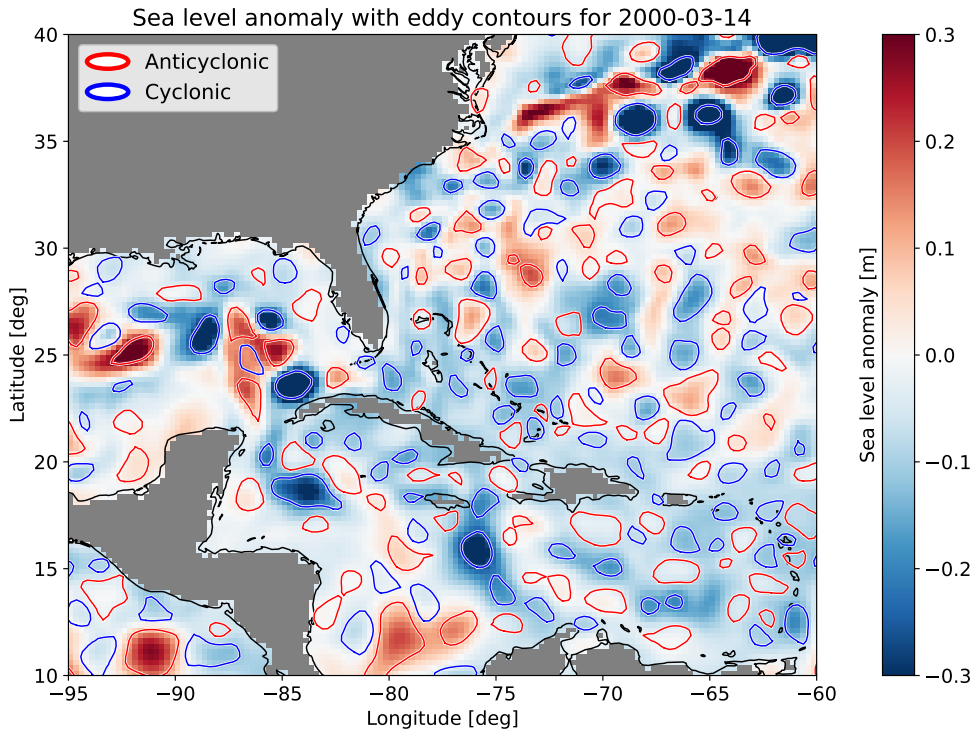5. Has amplitude, A, for which $1 \leq A \leq 150cm$

Figure 3.1: Sea level anomaly heatmap with eddy polygons obtained from the py-eddy-tracker overlaid

An example of the py-eddy-tracker in action is shown in Figure 3.1. The py-eddy-tracker tool was produced in 2014, and some of its shortcomings were identified in the work of Pegliasco et al. 2021 [32]. One notable difference in the outcome of the improved detection algorithm by Pegliasco et al. [32] is that it was slightly more accurate in detecting smaller eddies and trajectories lasting at least 10 days, in large data-sets. However, the improved version of the tracker was not available as a standalone tool, while the py-eddy-tracker was easily accessible via github with examples and tutorials, and was extensively

tested and utilised in previous published works – showing it can accurately detect mesoscale eddies even while having some space for improvements (Mason et al. 2019 [28], van der Boog et al. 2019 [1] etc.).

3.4. Data handling

To assemble the data in a comparable way and to reduce interpolation artefacts, the grid of the coarser dataset was chosen as reference grid, this being the SLA dataset – with cell size of 0.125°. This grid was used in the subsampling and interpolation of the chlorophyll data. Furthermore, as visualised in Figure 3.2 the data was assembled as follows:

- The data from CMEMS was collected via their online tooling (chlorophyll and SLA)

- The resulting chlorophyll measurements were subsampled by interpolation to the reference grid and stored

- The SLA data points were already on the reference grid, so they were stored

- To then extract the eddy information, the following process was employed:

    - The py-eddy-tracker was applied on the reference grid SLA to extract eddy polygons

    - These eddy polygons were used to determine if plastic was present in the eddy, by testing if the measurement coordinate falls within the polygon for each of the plastic data point in the combined dataset

    - In the case of presence, the eddy information was recorded, including: the eddy radius, the distance from center where plastic was detected, the eddy type (cyclonic/anticyclonic) as well as the total number of cyclonic/anticyclonic eddies on that day

- Finally, for each plastic data point, the SLA and chlorophyll were computed for the exact coordinate via interpolation over the reference grid

- The resulting assembled dataset was stored in NetCDF format

The above data processing steps were performed for each of the regions identified, these being:
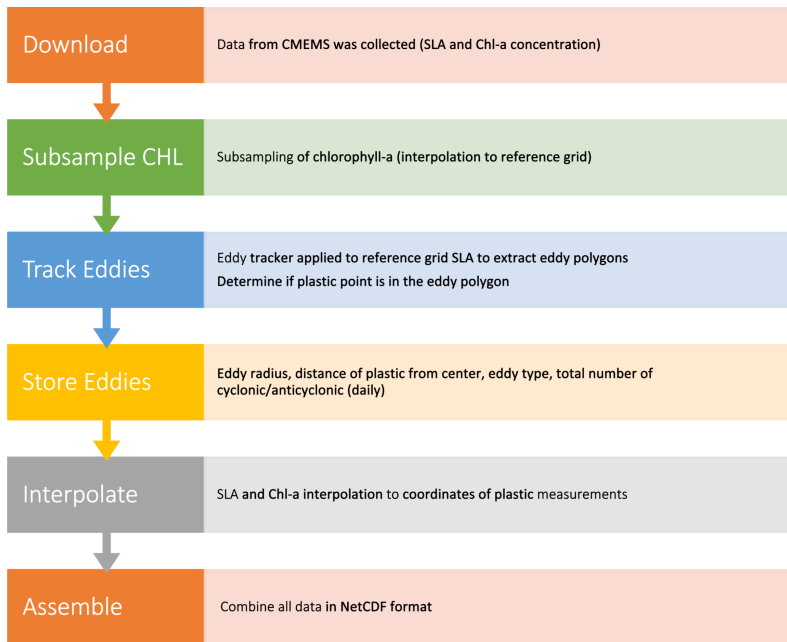
Figure 3.2: Visualisation of the data processing steps applied to the raw data

- North Atlantic (100°W to 10°W, 0°N to 60°N) (NA)

- South Atlantic (70°W to 20°E, 70°S to 0°S) (SA)

- North Pacific (180°W to 100°W, 0°N to 70°N) (NP)

- South Pacific (180°W to 80°W, 70°S to 0°S) (SP)

- Mediterranean (0°E to 40°E, 30°N to 50°N) (M)

- Indian Ocean (20°E to 180°E, 60°S to 0°S) (IO)

- Gulf Stream (80°W to 50°W, 26°N to 44°N) (GS)

- Global Ocean

where an individual dataset and its corresponding NetCDF file was produced for each of the regions of interest (the general location of these regions is shown in Figure 4.1). The distribution of data in each of the regions is visualized in Figure 3.3. The largest amount of measurement points fall in the North
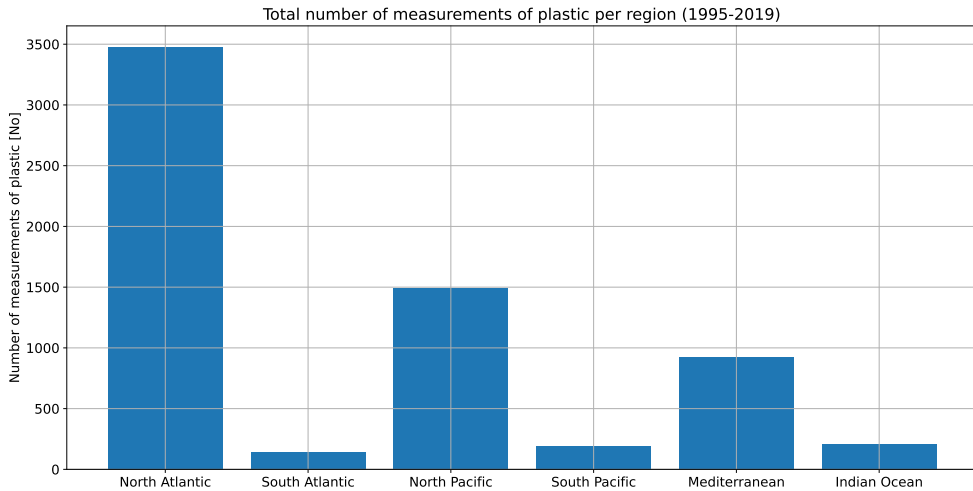
Figure 3.3: Plastic measurement count per region

Atlantic and North Pacific, with still a notable amount present in the Mediterranean. The remaining regions have a far smaller number of measurements present, which is in line with the general issues of the Southern hemisphere being sampled less (Suaria et al. 2020 [43]). Due to the lack of measurements present in the South Atlantic, South Pacific and the Indian Ocean, the analysis was centered around the North Atlantic and North Pacific, as well as a global picture. For the Mediterranean, there is a larger proportion of measurements than in the other regions where the analysis does not center on, but there is still not enough plastic measurements falling inside eddies to be able to perform a more robust and solid analysis (further details in section 4.2 and Figure 4.5b).

3.4.1. Data analysis methods

The analysis of the final data-set was performed in Python 3.7. This was done by loading the NetCDF into an xarray, and then analyzing the data with scatter plots, bar plots, histograms (with sample sum standard deviation), violin plots, linear regression fits, correlation calculation, as well as heatmaps and contour plots.

Results and Analysis

4.1. Extended data-set and seasonal data availability
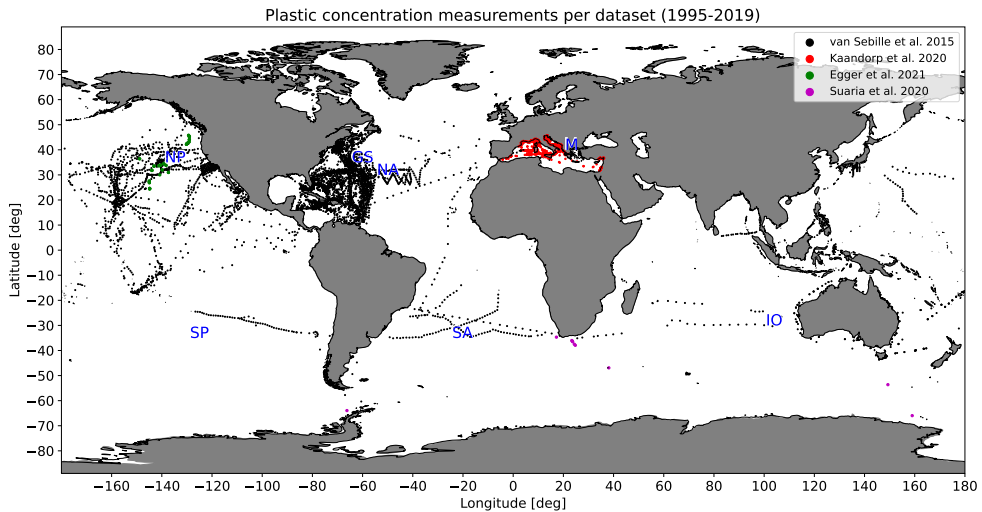

Figure 4.1: Plastic measurement locations in the world for each of the incorporated data-sets, with blue letters representing regions of interest

With the expansion of the core data-set described in section 3.1, the new date range now covers the years 1995 to 2019. The measurement locations from this expanded data-set are visualized in Figure 4.1. This visualization clearly shows the measurement gaps outside of the main regions, and especially in the Southern Hemisphere, as discussed in Section 1.1, where it is important to note that this issue is not helped by the data-set requirements imposed, as they are specific enough for many less data-strict studies to not fit them.

However, the resulting data-set is far more robust regardless, precisely due to the relatively strict rules under which it was constructed.
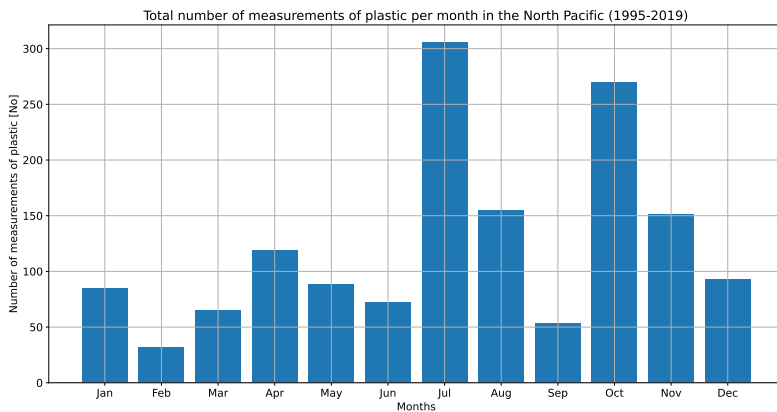
(a) Plastic measurements per month in the North Pacific
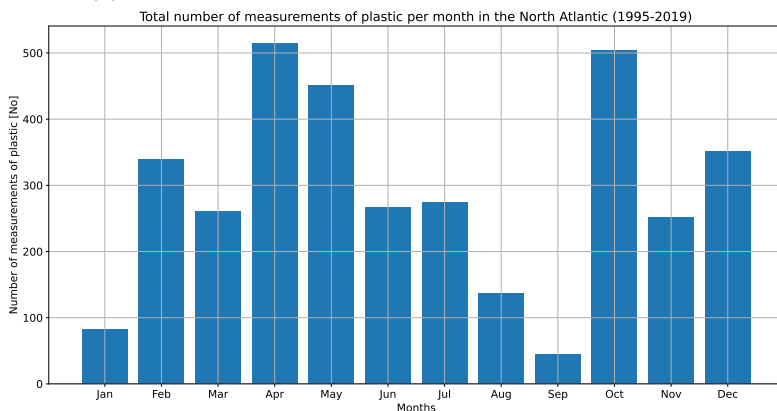
(b) Plastic measurements per month in the North Atlantic

Figure 4.2: Total plastic measurements per month in the two areas of interest: North Pacific (top) and North Atlantic (bottom).

In Figures 4.2a and 4.2b, we can observe the distribution of measurements per month, where each monthly bar represents the total number of measurements performed in that month between 1995 and 2019. What is immediately noticeable, is that the majority of measurements for the North Atlantic were performed in two time periods: between April and May as well as in October. Similarly, the majority of measurements for the North Pacific were done in the July and October.

One of the possible reasons for this, at least in the case of the North Atlantic, is that at least 20% of the measurements from the core data-set were taken by the SEA Data Collection [36]. This is of note because said data is collected on scheduled expeditions, and so we can match the peaks of measurements with the months where most of these expeditions happen, since the majority of the sampling is in the North Atlantic as well.

Due to observing these notable measurement peaks, a seasonal analysis is performed at the end of this chapter.

4.2. Eddy and plastic analysis

We will begin by observing the plastic concentration in eddies in our regions of interest (North Atlantic and North Pacific), as shown in Figure 4.3. The first thing that we can observe is that in the case of the North Atlantic there is 51.08 % of the plastic present in anticyclonic eddies, and only 8.36% can be found in cyclonic eddies, while 40.54% of all plastic measured did not fall within any type of eddy. On the other hand, in the case of the North Pacific, a total of 7.96% of plastic fell into anticyclonic, and 4.42% was found in cyclonic eddies, while the majority of the plastic (87.6%) was not in an eddy at all.

In contrast with the North Pacific, the fact that a significant amount of plastic was located within eddies in the case of the North Atlantic can be explained by the fact that most of the plastic samples were taken at the west part of the basin, where the Gulf Stream is found. The Gulf Stream is a notable eddy producer due to the instabilities of strongly horizontally sheared motions present within boundary currents (as per Section 2.2). The Gulf Stream also produces eddies roughly evenly (Kang et al. 2013 [20]), which is further supported by the number of plastic measurements within eddies in the North Atlantic – with 404 measurements being in anticyclonic eddies and 368 were within cyclonic ones. Furthermore, the vast majority of plastic found in eddies in the North Atlantic was located within anticyclonic eddies. This could be due to that anticyclonic eddies induce a surface flow inward and so produce an area of convergence, where floating plastic debris can accumulate.

While this rule also applied in the case of the North Pacific, on the other

(a) Anticyclonic case (North Atlantic)

(b) Cyclonic case (North Atlantic)

(c) Anticyclonic case (North Pacific)
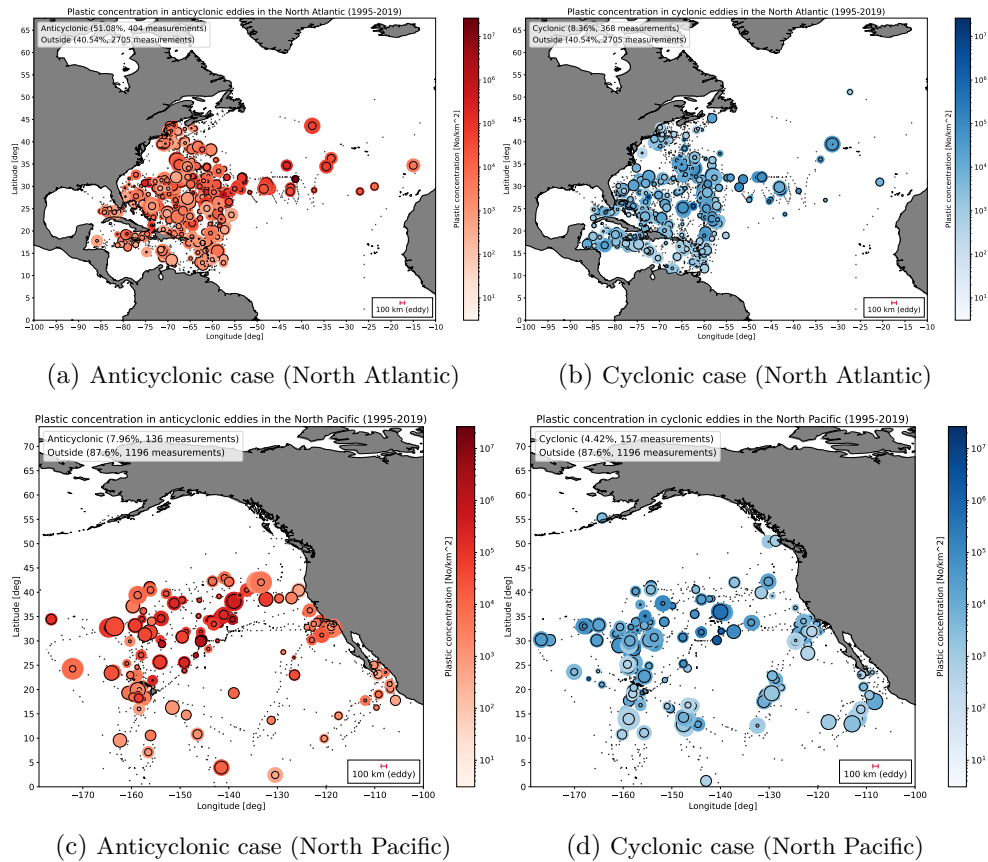
(d) Cyclonic case (North Pacific)

Figure 4.3: Plastic concentration in anticyclonic/cyclonic eddies in the regions of interest, with black dots representing plastic measurement points not falling within an eddy

hand, a far smaller amount of plastic is observed in eddies overall within this region. This is sensible due to the lower amount of kinetic energy available for eddy formation in the Pacific. In this case, the California boundary current is another notable eddy producer, where cyclonic eddies generally pinch off from meanders (Chelton et al. 2011 [4]) – however the eddy tracker does not do a good job with the detection when very close to the coastline, due to the (first Gaussian filtering) step of its algorithm. In spite of this, we still observe a cluster of eddies near the coastline in the California boundary current. Furthermore, the region northwest of Hawaii has a number of seamountchains,

which are capable of either rapid amplification of the westward propagating eddies, or Rossby waves from the eastern basin (as per Section 2.2). As a result a large cluster of cyclonic and anticylconic eddies (containing plastic), can be observed in this region.

Now, let us observe Figure A.2, where the distribution of eddies with plastic measurements are visualized globally. In this case, even when there is a predisposition for more cyclonic eddies worldwide (as per Section 2.2), we have independently verified that in our data-set, the distribution of cyclonic to anticyclonic eddies globally discovered by the eddy tracker was a near perfect 50/50 (within tolerance). This confirms that no additional conditional probability bias to eddy detection on the global scale is added, and as such no additional probability corrections based on their ratio are necessary. It is of note that in the global oceans, 13.8% of the plastic can be found in anticyclonic eddies, 4.08% in cyclonic ones, and 82.11% is not found in eddies at all.

In Figure 4.5 we can observe the histograms of summed plastic counts divided by total number of measurement per region and eddy type. We can immediately notice that the pattern of more plastic being located in anticyclonic eddies applies to the the North Atlantic, North Pacific, South Pacific and the Mediterranean. However, in the Mediterranean even though it is the third region with most data, there are not enough plastic measurements within eddies for this result to be robust (Figure 4.5b), in addition to the tracker having a bias towards detecting cyclonic eddies there (Stegner et al. 2021 [41]). Furthermore, the Rossby radius of deformation is lower in the Mediterranean than in the Atlantic and Pacific Ocean at the same latitude, making it so that the actual eddies observed are smaller, especially in the case of the cyclonic eddies, which are less stable and often split up into sub-mesoscale structures having a rapid dynamical evolution – which is not well captured by gridded SLA data in the first place (Stegner et al. 2021 [41]).

Additionally, there is so few measurement points for the South Pacific, South Atlantic and Indian Ocean that we cannot make any meaningful conclusions there (see Figure 3.3). The histogram also further supports the known fact that the Gulf Stream is a notable equal parts eddy producer (Kang et al. 2013 [20]), as most of the plastic sampling points are found in eddies, and the split is quite even.
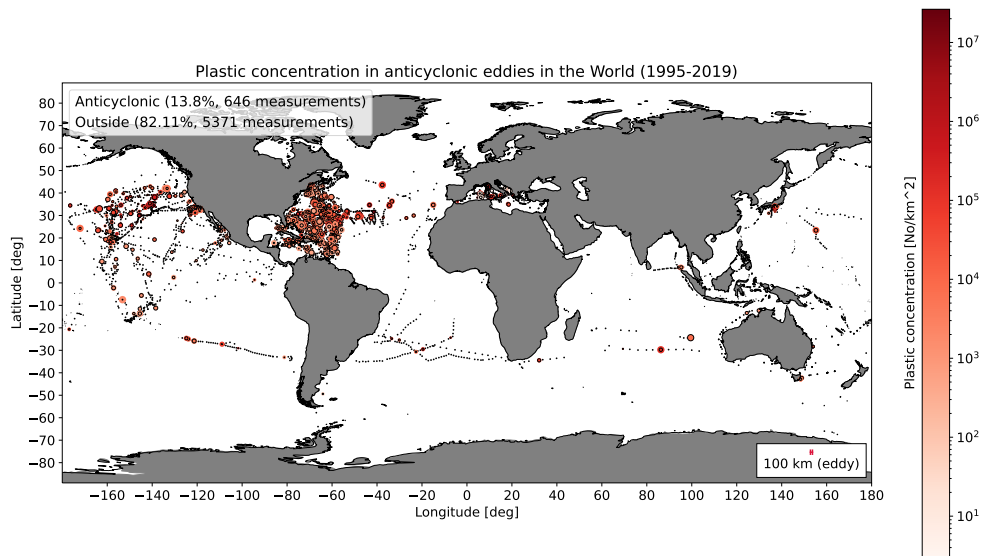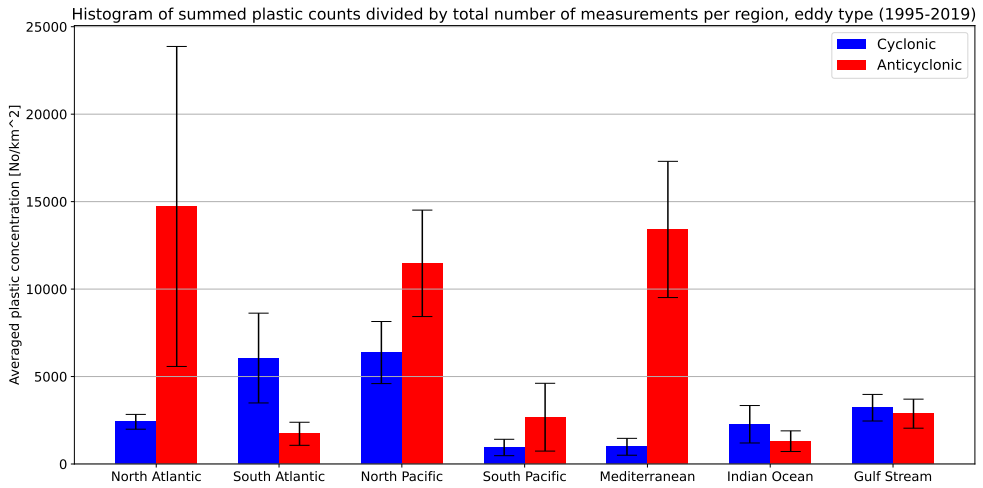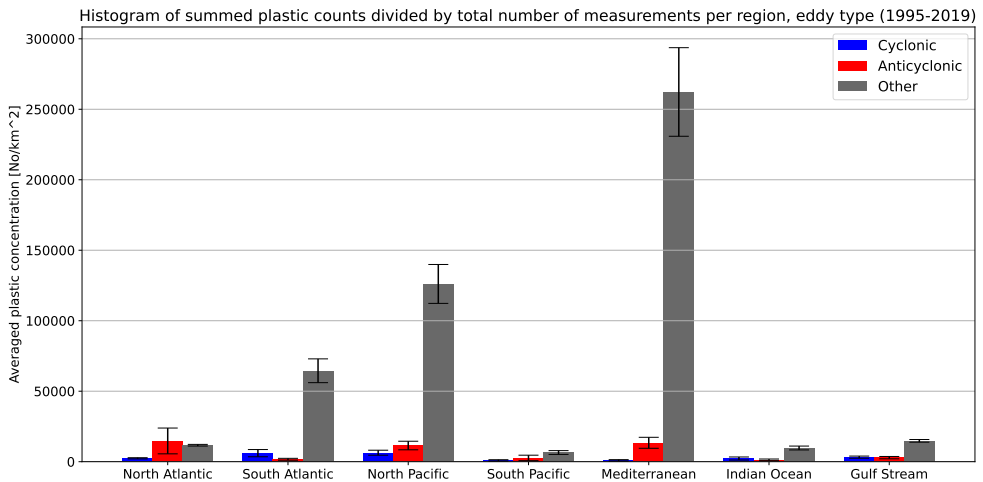
(a) Anticyclonic case
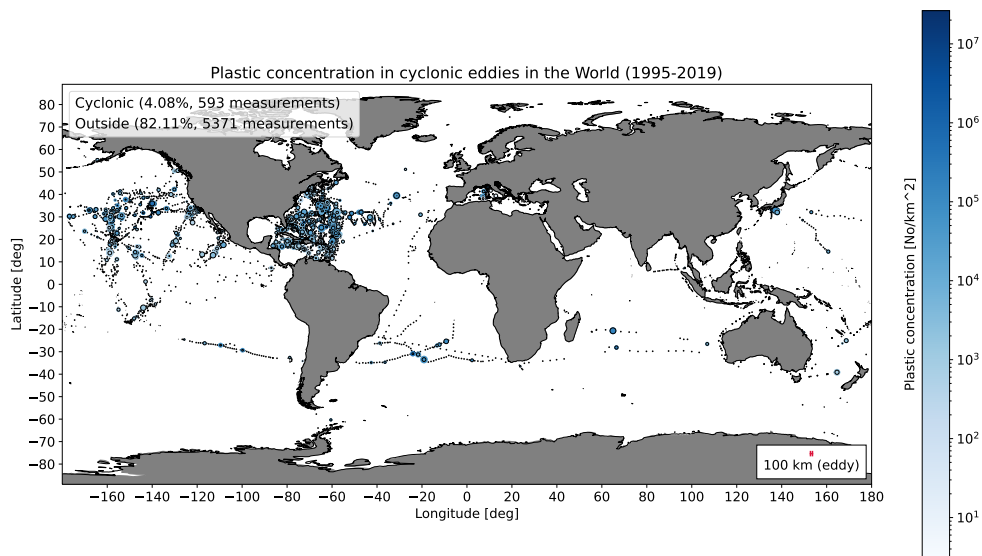
(b) Cyclonic case

Figure 4.4: Plastic concentration in anticyclonic/cyclonic eddies in the World

(a) Anticyclonic/Cyclonic only

(b) All data case

Figure 4.5: Histogram of summed plastic counts divided by total number of measurements per region, eddy type. The error bars were computed as the standard deviation of a sum of values using the formula $\sqrt{n} * \sigma$, where σ is the standard deviation of the measurements, and n is the number of samples.

Figure 4.6 shows the distribution of plastic concentration per region by eddy type. We can notice that in the case of the Gulf Stream, both cyclonic
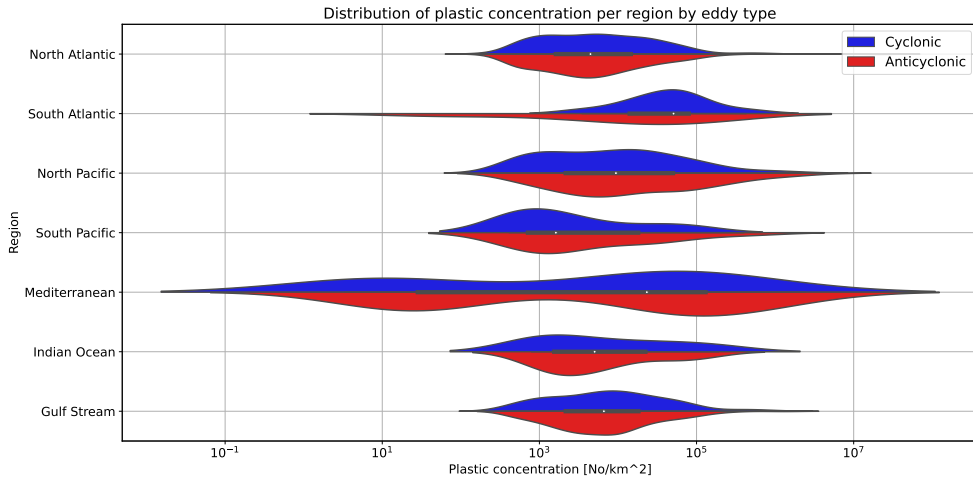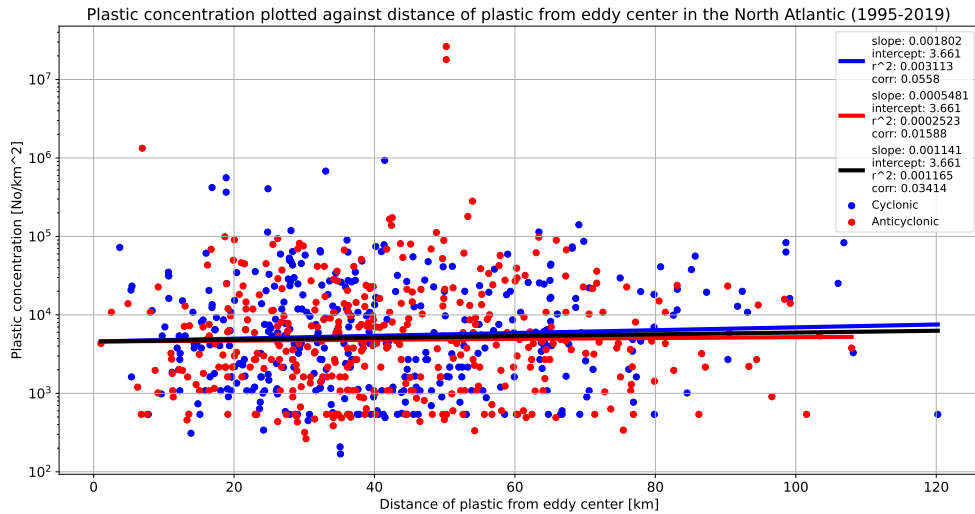
Figure 4.6: Distribution of plastic concentration per region by eddy type (log scale plastic concentration)

and anticyclonic eddies have a similar distribution of plastic concentration. On the other hand, the log distribution of the North Pacific has a longer and wider right tail than that of the North Atlantic, indicating that there are more samples with a high value of plastic concentration there, while the left tails of these distributions are comparable. This is consistent with the Great Pacific Garbage Patch being the larger one in comparison to the plastic accumulated in the other ocean gyres (Ocean Cleanup Project [35]). Also of note is that the Mediterranean has a bi-modal distribution, with large tails on both sides – indicating that the plastic concentration measurements were either very large or very small at each measured point when within eddies, and with anticyclonic leading with the right mode, as expected from previous conclusions. Additionally of interest are the modes of the plastic within anticyclonic eddies in the North Atlantic and North Pacific, which are both roughly within the plastic concentration value.

Figure 4.7 shows plastic concentration is plotted against eddy radius as well as distance of plastic from the eddy center for the North Atlantic. From the linear regression fit (assessed by the goodness-of-fit parameter, R^2) and the correlation coefficient (corr.) (shown in the legend of Figure 4.7a), we can only conclude that there is no correlation between plastic concentration and distance of plastic from eddy center. Also, no correlation between plastic
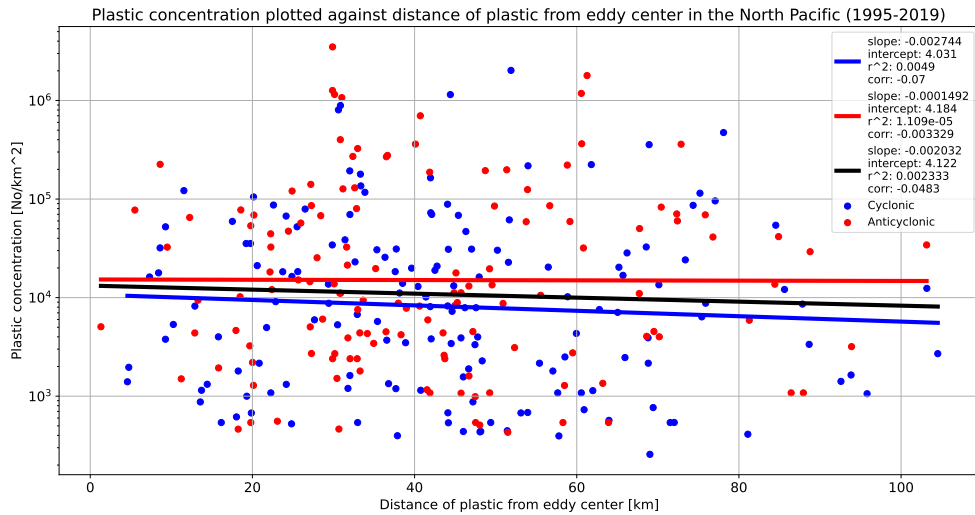
(a) Distance of plastic from eddy center
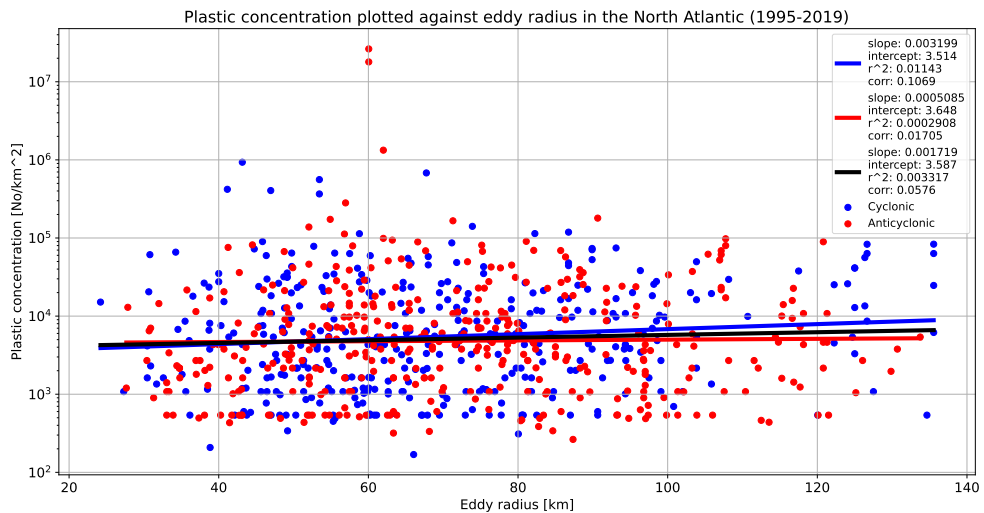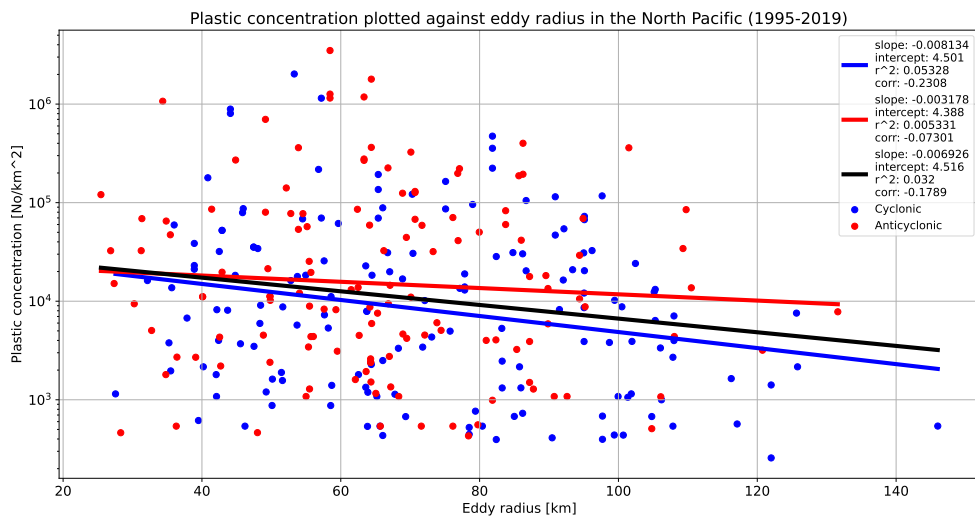

(b) Eddy radius

Figure 4.7: Plastic concentration plotted against eddy variables in the North Atlantic. The lines correspond to fits done over points in all eddies (black line), cyclonic eddies alone (blue line) and anticyclonic alone (red line), respectively.

concentration and eddy radius for the North Atlantic was found. Even when

considering the separate fits of cyclonic and anticyclonic regression lines – no correlation is observed there either.

(a) Distance of plastic from eddy center

(b) Eddy radius

Figure 4.8: Plastic concentration plotted against eddy variables in the North Pacific

Let us now observe Figure 4.8, where plastic concentration is plotted against eddy radius as well as distance of plastic from the eddy center for the North Pacific. Just as with the North Atlantic, no correlation can be observed in this case either. One would expect that having a bigger eddy would correlate with a larger plastic concentration, however due to sparsity of data points on a global scale it is unlikely that such a pattern would emerge without further data and analysis. One other alternative possibility is to observe the extremes of this distribution in the case two modes are present, as in, it could be possible that there are a few bigger eddies with a lot of plastic, or many smaller eddies with little plastic in them, but this will not be explored further here. Once again though, less eddies are present in the Pacific, due to most measurements in the Pacific being taken in the eastern part of the basin, where there is less kinetic energy, which further brings down the number of measurement points for eddies.

4.3.   Seasonal variability

As discussed in Section 4.1, the data in the North Atlantic and North Pacific is highly seasonal, so it is interesting to explore the two main month ranges for each of these regions.

In the case of the North Atlantic, the two time spans of interest are visualized in Figure 4.9. The first thing of note here is to notice that in the time range of April-May, most of the data points fall within the Gulf Stream, so we get a similar number of plastic samples falling in cyclonic and anticyclonic eddies (96 and 113, respectively), and comparable plastic concentration percentages. In the case of the October time range, the data is mostly covering the gyre, so the proportion of plastic concentration in anticyclonic eddies is greater than that of cyclonic eddies. This can be explained by the fact that the gyre does not have well-defined boundaries, and so the data points are entering the North Equatorial current. The measurement points are also overall positioned closer to the open ocean, and so more energy is dissipated. This further implies that anticyclonic eddies, which have a larger travel distance and longevity than their cyclonic counterparts (Chelton et al. 2011 [4]), can trap more plastic than shorter lived and smaller cyclonic eddies as per Section 2.2.

(a) Anticyclonic case (Apr-May)

(b) Cyclonic case (April-May)

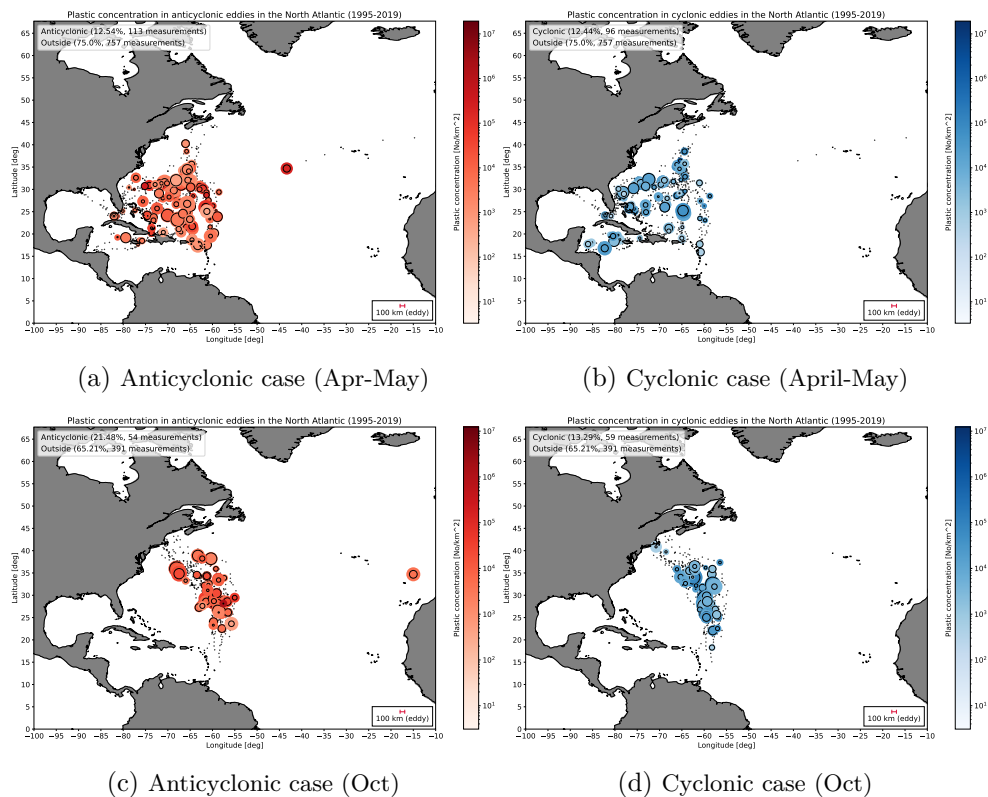(c) Anticyclonic case (Oct)

(d) Cyclonic case (Oct)

Figure 4.9: Plastic concentration in anticyclonic/cyclonic eddies in the North Atlantic

In the case of the North Pacific however, the same rules and proportions as noted in previous sections are followed in the seasonal case as well (Figure 4.10).

4.4. Chlorophyll and plastic analysis

As discussed in the theoretical background (Section 2.2), high concentrations of chlorophyll were often observed at the core of cyclonic eddies, and the opposite was true for anticyclonic ones, which can be attributed to the upwelling in cyclonic eddies, which brings up nutrients from lower layers of the ocean, thus allowing algal cells to flourish. The same pattern was observed in the extended data-set as well, as seen in Figure 4.11, where the highest value

(a) Anticyclonic case (Jul)

(b) Cyclonic case (Oct)

(c) Anticyclonic case (Oct)
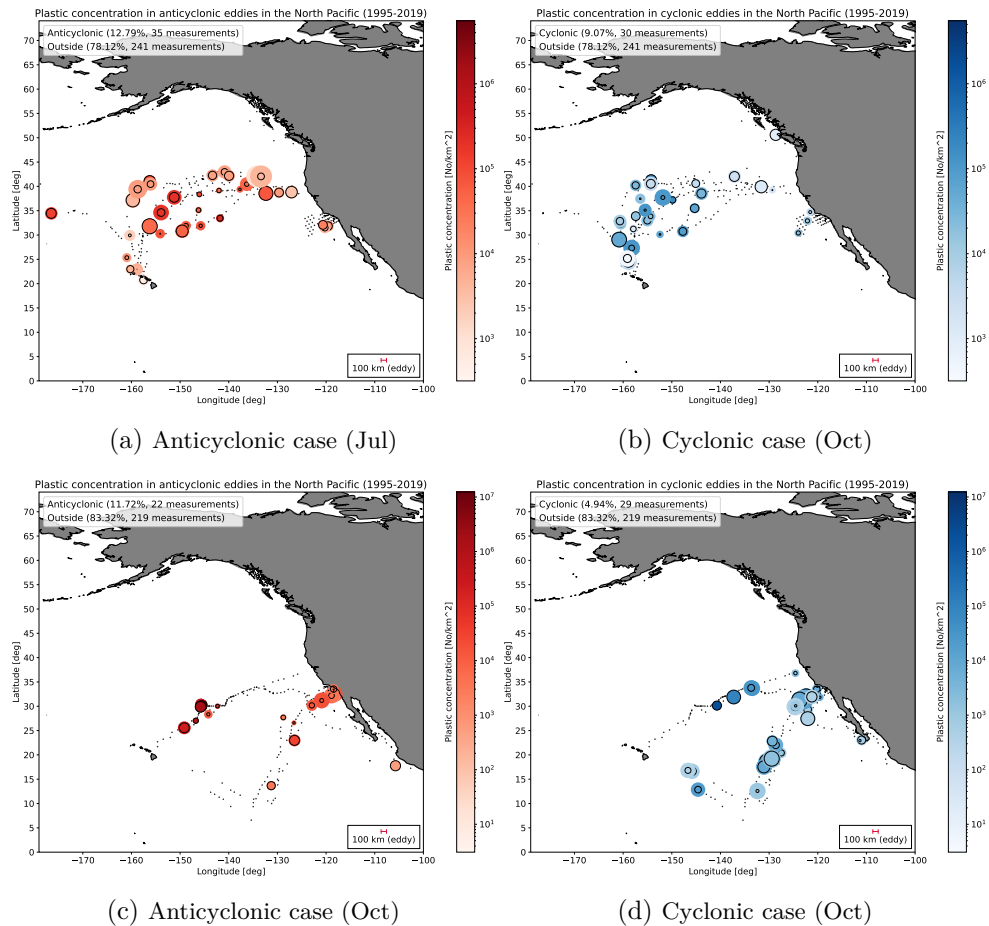
(d) Cyclonic case (Oct)

Figure 4.10: Plastic concentration in anticyclonic/cyclonic eddies in the North Pacific

chlorophyll points are predominantly cyclonic.

On the other hand, the largest amount of plastic is present in anticyclonic eddies. These two facts together lead to two possible consequences. The first possibility is that biofouling is stronger in cyclonic eddies, and so plastic sinks, resulting in less plastic in cyclonic eddies (Lobelle et al. 2021 [27]). Alternatively, due to smaller plastic concentration in cyclonic eddies, less plastic is available for biofouling, even though chlorophyll concentration is high. In the case of the latter possible consequence being the valid one, this would be pos-
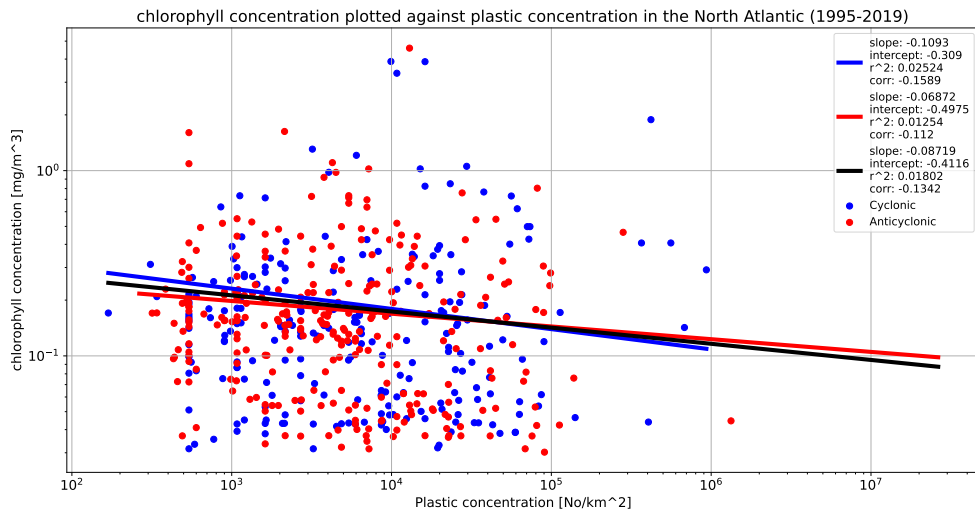
(a) North Atlantic region
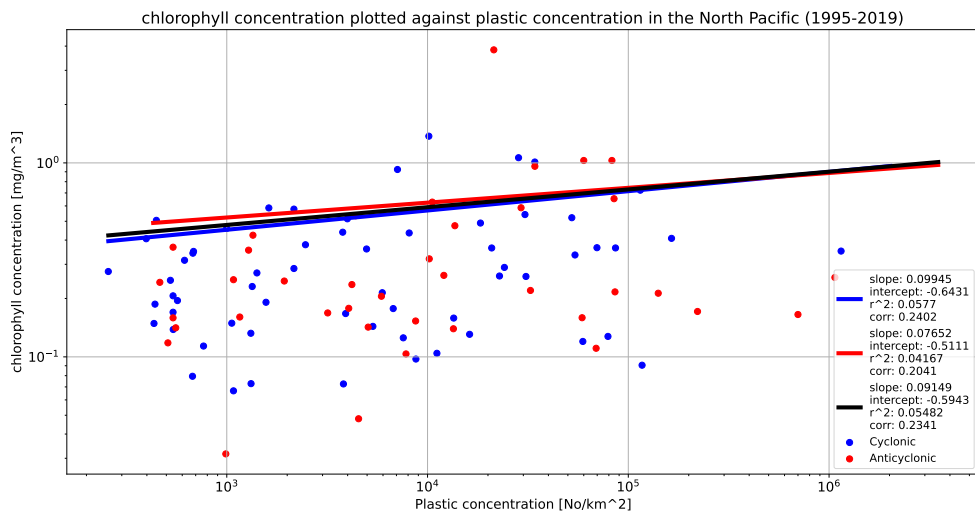
(b) North Pacific region

Figure 4.11: Chlorophyll concentration plotted against plastic concentration in the regions of interest

itive news for the environmental impact of marine plastic on biodiversity, due to this option resulting in less plastic being consumed by biota.

Conclusions

In this work we have explored the possible relationships between marine microplastic, mesoscale eddies and chlorophyll, with the goal of answering the research questions posed in Section 1.2. These questions were addressed, and the first notable conclusion that was derived, is that higher microplastic concentrations were present in anticyclonic eddies when compared to plastic present in cyclonic eddies. This was observed in all major regions of research (North Atlantic and North Pacific), where there was sufficient data available to draw meaningful conclusions. However, the remaining regions had very sparse data available making it impossible to make truly large scale conclusions. Anticyclonic mesoscale eddies were observed to accumulate more surface microplastic than cyclonic eddies, and this could be due to the surface inward flow of anticyclonic eddies. The lower plastic concentration observed in cyclonic eddies could be explained by the process of biofouling, that could make the plastic particles sink. Moreover, if less plastic actually accumulates in cyclones than anticyclones, and not just less being observed because of sinking due to biofouling, this would fortunately mean that plastic could pose a smaller risk to the marine environment as the majority of the plastic lies within anticyclonic eddies (where there is usually less biological activity). Furthermore, no relationship between plastic concentration and eddy radius or distance from center of eddy was observed. The plastic concentration was analysed seasonally in the North Atlantic and North Pacific. Here the seasonal paths of the ships from which the measurements were carried out had an impact on the outcome of the seasonal analysis, as it only gave a partial image of the local area. Finally, the results found in this research study help shed some light on the impact of mesoscale eddies on the distribution of marine microplastics, which is important in understanding plastic dynamics in the ocean and its impact on the marine environment.

Future Work

Due to some of the data related difficulties identified over the course of the previous chapters, a number of avenues for future work exist. Firstly, in addition to the data-set assembly done in this thesis, one possibility is to apply a model based normalization to the data, with a mathematical model such as the general additive model (GAM). Such a model could be applied using wind speed, longitude and latitude, among other additional inputs to model the global spread of plastic – and then the outputs of the model could be determined for the original plastic measurements, and used as a form of "standardized" plastic data-set (similar to the work done by van Sebille et al. [37]).

More than half of the areas of interest explored in this paper had a significant lack of marine plastic measurements. This is a known problem with marine plastic sampling (Suaria et al. 2020 [43]), where even the Mediterranean, where more data was available, has a relatively small representation overall. On top of that, the entire Southern hemisphere is very poorly represented (Suaria et al. 2020 [43]). With this in mind, a global, virtual plastic distribution simulation (like in for example [37]) could be a good tool to patch the data, and possibly allow us to explore the undermeasured areas in more depth. With a plastic distribution simulation, the analysis performed in this thesis could be reproduced and compared to our results to derive further conclusions. This approach could also address the lack of precision of the plastic data-set due to a ranging variety in sampling methods and there being no cohesive standardization on the plastic measurements.

Finally, a possible extension to the work, would be to use other algorithms/tools for tracking eddies, and compare the output to the analysis pre-

sented here to further confirm our conclusions. This could help reduce the impact of any bias present in the eddy tracking tool used on the conclusions obtained.

Bibliography

[1] C. G. van der Boog et al. "Hydrographic and Biological Survey of a Surface-Intensified Anticyclonic Eddy in the Caribbean Sea". In: *Journal of Geophysical Research: Oceans* 124.8 (2019), pp. 6235–6251. DOI: https://doi.org/10.1029/2018JC014877. eprint: https://agupubs.onlinelibrary.wiley.com/doi/pdf/10.1029/2018JC014877. URL: https://agupubs.onlinelibrary.wiley.com/doi/abs/10.1029/2018JC014877.

[2] Laurent Brach et al. "Anticyclonic eddies increase accumulation of microplastic in the North Atlantic subtropical gyre". In: *Marine Pollution Bulletin* 126 (2018), pp. 191–196. ISSN: 0025-326X. DOI: https://doi.org/10.1016/j.marpolbul.2017.10.077. URL: https://www.sciencedirect.com/science/article/pii/S0025326X17309232.

[3] Øyvind Breivik et al. "Advances in search and rescue at sea". In: *Ocean Dynamics* 63.1 (2013), pp. 83–88. ISSN: 1616-7228. DOI: 10.1007/s10236-012-0581-1. URL: https://doi.org/10.1007/s10236-012-0581-1.

[4] Dudley B. Chelton, Michael G. Schlax, and Roger M. Samelson. "Global observations of nonlinear mesoscale eddies". In: *Progress in Oceanography* 91.2 (2011), pp. 167–216. ISSN: 0079-6611. DOI: https://doi.org/10.1016/j.pocean.2011.01.002. URL: https://www.sciencedirect.com/science/article/pii/S0079661111000036.

[5] Dudley B. Chelton et al. "Global observations of large oceanic eddies". In: *Geophysical Research Letters* 34.15 (2007). DOI: https://doi.org/10.1029/2007GL030812. eprint: https://agupubs.onlinelibrary.wiley.com/doi/pdf/10.1029/2007GL030812. URL: https://agupubs.onlinelibrary.wiley.com/doi/abs/10.1029/2007GL030812.

[6] Copernicus Marine Environment Monitoring Service (CMEMS). *OCEANCOLOUR-GLO-CHL-L4-REP-OBSERVATIONS-009-082 product*. https://resources.marine.copernicus.eu/product-detail/OCEANCOLOUR_GLO_CHL_L4_REP_OBSERVATIONS_009_082/INFORMATION. [Online; accessed 19-Nov-2021]. 2021.

[7] Copernicus Marine Environment Monitoring Service (CMEMS). *SEALEVEL-GLO-PHY-L4-REP-OBSERVATIONS-008-047-TDS product*. https://resources.marine.copernicus.eu/product-detail/SEALEVEL_GLO_PHY_L4_REP_OBSERVATIONS_008_047/INFORMATION. [Online; accessed 19-Nov-2021]. 2021.

[8] Scott Condie and Ryan Condie. "Retention of plankton within ocean eddies". In: *Global Ecology and Biogeography* 25.10 (2016), pp. 1264–1277. DOI: https://doi.org/10.1111/geb.12485. eprint: https://onlinelibrary.wiley.com/doi/pdf/10.1111/geb.12485. URL: https://onlinelibrary.wiley.com/doi/abs/10.1111/geb.12485.

[9] Matthias Egger et al. "Relative Abundance of Floating Plastic Debris and Neuston in the Eastern North Pacific Ocean". In: *Frontiers in Marine Science* 8 (2021), p. 566. ISSN: 2296-7745. DOI: 10.3389/fmars.2021.626026. URL: https://www.frontiersin.org/article/10.3389/fmars.2021.626026.

[10] Marcus Eriksen et al. "Plastic pollution in the South Pacific subtropical gyre". In: *Marine Pollution Bulletin* 68.1 (2013), pp. 71–76. ISSN: 0025-326X. DOI: https://doi.org/10.1016/j.marpolbul.2012.12.021. URL: https://www.sciencedirect.com/science/article/pii/S0025326X12006224.

[11] G. Everaert et al. "Risks of floating microplastic in the global ocean". In: *Environmental Pollution* 267 (2020), p. 115499. ISSN: 0269-7491. DOI: https://doi.org/10.1016/j.envpol.2020.115499. URL: https://www.sciencedirect.com/science/article/pii/S026974912036187X.

[12] James H. Faghmous et al. "A daily global mesoscale ocean eddy dataset from satellite altimetry". In: *Scientific Data* 2.1 (2015), p. 150028. ISSN: 2052-4463. DOI: 10.1038/sdata.2015.28. URL: https://doi.org/10.1038/sdata.2015.28.

[13] Peter Gaube et al. "Regional variations in the influence of mesoscale eddies on near-surface chlorophyll". In: *Journal of Geophysical Research: Oceans* 119.12 (2014), pp. 8195–8220. DOI: https://doi.org/10.

1002/2014JC010111. eprint: https://agupubs.onlinelibrary.wiley.com/doi/pdf/10.1002/2014JC010111. URL: https://agupubs.onlinelibrary.wiley.com/doi/abs/10.1002/2014JC010111.

[14] Jamison M. Gove et al. "Prey-size plastics are invading larval fish nurseries". In: *Proceedings of the National Academy of Sciences* 116.48 (2019), pp. 24143–24149. ISSN: 0027-8424. DOI: 10.1073/pnas.1907496116. eprint: https://www.pnas.org/content/116/48/24143.full.pdf. URL: https://www.pnas.org/content/116/48/24143.

[15] Qingyou He et al. "Phytoplankton bloom triggered by an anticyclonic eddy: The combined effect of eddy-Ekman pumping and winter mixing". In: *Journal of Geophysical Research: Oceans* 112 (June 2017). DOI: 10.1002/2017JC012763.

[16] Nauzet Hernández-Hernández et al. "Drivers of Plankton Distribution Across Mesoscale Eddies at Submesoscale Range". In: *Frontiers in Marine Science* 7 (2020), p. 667. ISSN: 2296-7745. DOI: 10.3389/fmars.2020.00667. URL: https://www.frontiersin.org/article/10.3389/fmars.2020.00667.

[17] Xueyan Hou et al. "Seasonal and interannual variability of chlorophyll-a and associated physical synchronous variability in the western tropical Pacific". In: *Journal of Marine Systems* 158 (2016), pp. 59–71. ISSN: 0924-7963. DOI: https://doi.org/10.1016/j.jmarsys.2016.01.008. URL: https://www.sciencedirect.com/science/article/pii/S092479631600021X.

[18] Langmuir I. "Surface motion of water induced by wind Science". In: 87 (1938), 119–23.

[19] Mikael L. A. Kaandorp, Henk A. Dijkstra, and Erik van Sebille. "Closing the Mediterranean Marine Floating Plastic Mass Budget: Inverse Modeling of Sources and Sinks". In: *Environmental Science & Technology* 54.19 (2020). PMID: 32852202, pp. 11980–11989. DOI: 10.1021/acs.est.0c01984. eprint: https://doi.org/10.1021/acs.est.0c01984. URL: https://doi.org/10.1021/acs.est.0c01984.

[20] Dujuan Kang and Enrique N. Curchitser. "Gulf Stream eddy characteristics in a high-resolution ocean model". In: *Journal of Geophysical Research: Oceans* 118.9 (2013), pp. 4474–4487. DOI: https://doi.org/10.1002/jgrc.20318. eprint: https://agupubs.onlinelibrary.wiley.com/doi/pdf/10.1002/jgrc.20318. URL: https://agupubs.onlinelibrary.wiley.com/doi/abs/10.1002/jgrc.20318.

[21] La Daana K. Kanhai et al. "Microplastic abundance, distribution and composition along a latitudinal gradient in the Atlantic Ocean". In: *Marine Pollution Bulletin* 115.1 (2017), pp. 307–314. ISSN: 0025-326X. DOI: https://doi.org/10.1016/j.marpolbul.2016.12.025. URL: https://www.sciencedirect.com/science/article/pii/S0025326X16310116.

[22] Timothy W. Kao, Fuh-Shing Pan, and Dominique Renouard. "Internal solitons on the pycnocline: generation, propagation, and shoaling and breaking over a slope". In: *Journal of Fluid Mechanics* 159 (1985), 19–53. DOI: 10.1017/S0022112085003081.

[23] Shinya Kouketsu et al. "Mesoscale eddy effects on temporal variability of surface chlorophyll a in the Kuroshio Extension". In: *Journal of Oceanography* 72.3 (2016), pp. 439–451. ISSN: 1573-868X. DOI: 10.1007/s10872-015-0286-4. URL: https://doi.org/10.1007/s10872-015-0286-4.

[24] Kara Law et al. "Plastic Accumulation in the North Atlantic Subtropical Gyre". In: *Science (New York, N.Y.)* 329 (Sept. 2010), pp. 1185–8. DOI: 10.1126/science.1192321.

[25] Pasadena CA USA Lee-Lueng Fu | Jet Propulsion Laboratory California Institute of Technology et al. "Eddy Dynamics from Satellite Altimetry". In: *Oceanography* issue$_v$olume (2010). URL: https://doi.org/10.5670/oceanog.2010.02.

[26] Sophie Leterme and Robin Pingree. "The Gulf Stream, rings and North Atlantic eddy structures from remote sensing (Altimeter and SeaW-iFS)". In: *Journal of Marine Systems* 69 (Feb. 2008), pp. 177–190. DOI: 10.1016/j.jmarsys.2005.11.022.

[27] Delphine Lobelle et al. "Global Modeled Sinking Characteristics of Bio-fouled Microplastic". In: *Journal of Geophysical Research: Oceans* 126.4 (2021). e2020JC017098 2020JC017098, e2020JC017098. DOI: https://doi.org/10.1029/2020JC017098. eprint: https://agupubs.onlinelibrary.wiley.com/doi/pdf/10.1029/2020JC017098. URL: https://agupubs.onlinelibrary.wiley.com/doi/abs/10.1029/2020JC017098.

[28] E. Mason et al. "New insight into 3-D mesoscale eddy properties from CMEMS operational models in the western Mediterranean". In: *Ocean Science* 15.4 (2019), pp. 1111–1131. DOI: 10.5194/os-15-1111-2019. URL: https://os.copernicus.org/articles/15/1111/2019/.

[29] Evan Mason, Ananda Pascual, and James C. McWilliams. "A New Sea Surface Height–Based Code for Oceanic Mesoscale Eddy Tracking". In: *Journal of Atmospheric and Oceanic Technology* 31.5 (2014), pp. 1181–1188. DOI: 10.1175/JTECH-D-14-00019.1. URL: https://journals.ametsoc.org/view/journals/atot/31/5/jtech-d-14-00019_1.xml.

[30] R. Onken and B. Baschek. "Properties and evolution of a submesoscale cyclonic spiral". In: *Ocean Science Discussions* 2021 (2021), pp. 1–51. DOI: 10.5194/os-2021-86. URL: https://os.copernicus.org/preprints/os-2021-86/.

[31] OpenLearn. *Open Learn Ocean Currents , Chapter 4.4.* https://www.open.edu/openlearn/science-maths-technology/the-oceans/content-section-4.4. [Online; accessed 19-Nov-2021]. 2021.

[32] C. Pegliasco et al. "META3.1exp : A new Global Mesoscale Eddy Trajectories Atlas derived from altimetry". In: *Earth System Science Data Discussions* 2021 (2021), pp. 1–31. DOI: 10.5194/essd-2021-300. URL: https://essd.copernicus.org/preprints/essd-2021-300/.

[33] Jesús Pineda. "An internal tidal bore regime at nearshore stations along western U.S.A.: Predictable upwelling within the lunar cycle". In: *Continental Shelf Research* 15.8 (1995), pp. 1023–1041. ISSN: 0278-4343. DOI: https://doi.org/10.1016/0278-4343(95)80007-Z. URL: https://www.sciencedirect.com/science/article/pii/027843439580007Z.

[34] Marie Poulain et al. "Small Microplastics As a Main Contributor to Plastic Mass Balance in the North Atlantic Subtropical Gyre". In: *Environmental Science & Technology* 53.3 (2019), pp. 1157–1164. DOI: 10.1021/acs.est.8b05458. eprint: https://doi.org/10.1021/acs.est.8b05458. URL: https://doi.org/10.1021/acs.est.8b05458.

[35] Ocean Cleanup Project. *The Great Pacific Garbage Patch.* https://theoceancleanup.com/great-pacific-garbage-patch/. [Online; accessed 19-Nov-2021]. 2021.

[36] Environmental Studies at Woods Hall Sea Education Association and at Sea. *SEA Data Collection.* https://www.sea.edu/SEA_Research/sea-data-access. [Online; accessed 20-Nov-2021]. 2021.

[37] Erik van Sebille et al. "A global inventory of small floating plastic debris". In: *Environmental Research Letters* 10.12 (2015), p. 124006. DOI: 10.1088/1748-9326/10/12/124006. URL: https://doi.org/10.1088/1748-9326/10/12/124006.

[38]   Erik van Sebille et al. "The physical oceanography of the transport of floating marine debris". In: *Environmental Research Letters* 15.2 (2020), p. 023003. DOI: 10.1088/1748-9326/ab6d7d. URL: https://doi.org/10.1088/1748-9326/ab6d7d.

[39]   Alan L. Shanks et al. "Demonstration of the onshore transport of larval invertebrates by the shoreward movement of an upwelling front". In: *Limnology and Oceanography* 45.1 (2000), pp. 230–236. DOI: https://doi.org/10.4319/lo.2000.45.1.0230. eprint: https://aslopubs.onlinelibrary.wiley.com/doi/pdf/10.4319/lo.2000.45.1.0230. URL: https://aslopubs.onlinelibrary.wiley.com/doi/abs/10.4319/lo.2000.45.1.0230.

[40]   Peter Sherman and Erik van Sebille. "Modeling marine surface microplastic transport to assess optimal removal locations". In: *Environmental Research Letters* 11.1 (2016), p. 014006. DOI: 10.1088/1748-9326/11/1/014006. URL: https://doi.org/10.1088/1748-9326/11/1/014006.

[41]   Alexandre Stegner, Briac Vu, and Franck Dumas. "Cyclone-Anticyclone Asymmetry of Eddy Detection on Gridded Altimetry Product in the Mediterranean Sea". In: *Journal of Geophysical Research: Oceans* 126 (Sept. 2021). DOI: 10.1029/2021JC017475.

[42]   G.G. Stokes. "On the Theory of Oscillatory Waves". In: *Transactions of the Cambridge Philosophical Society* 8 (1837), pp. 441–455.

[43]   Giuseppe Suaria et al. "Floating macro- and microplastics around the Southern Ocean: Results from the Antarctic Circumnavigation Expedition". In: *Environment International* 136 (2020), p. 105494. ISSN: 0160-4120. DOI: https://doi.org/10.1016/j.envint.2020.105494. URL: https://www.sciencedirect.com/science/article/pii/S0160412019335962.

[44]   Fabián J Tapia et al. "High-frequency observations of wind-forced onshore transport at a coastal site in Baja California". In: *Continental Shelf Research* 24.13 (2004), pp. 1573–1585. ISSN: 0278-4343. DOI: https://doi.org/10.1016/j.csr.2004.03.013. URL: https://www.sciencedirect.com/science/article/pii/S0278434304000652.

[45]   Richard Williams. "OceanographyOcean eddies and plankton blooms". In: *Nature Geoscience - NAT GEOSCI* 4 (Oct. 2011), pp. 739–740. DOI: 10.1038/ngeo1307.

[46]   Enrico Zambianchi et al. "Marine litter in the Mediterranean Sea: an oceanographic perspective". In: June 2014, 180 p. DOI: 10.13140/RG.2.1.2315.3760.
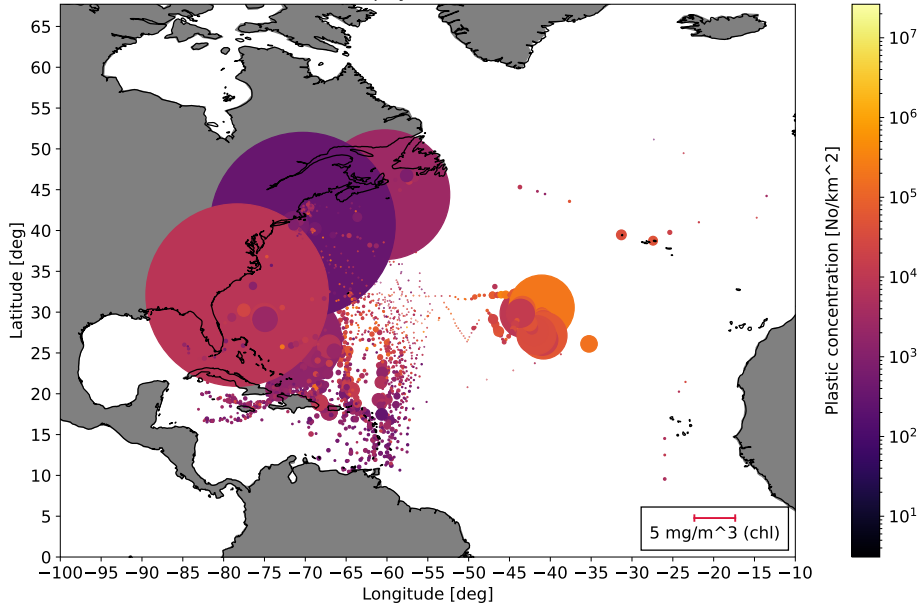
Appendix

A.1. Supplementary plots

A.2. Software

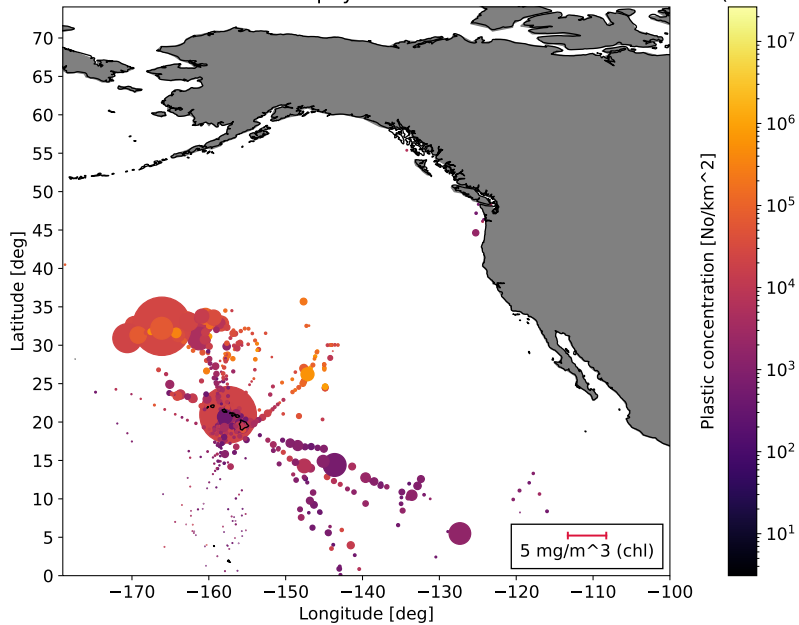A github repository was created including the necessary processing and analysis code used in this study (parcels team private repositpry): https://github.com/OceanParcels/EddyAccumulation.
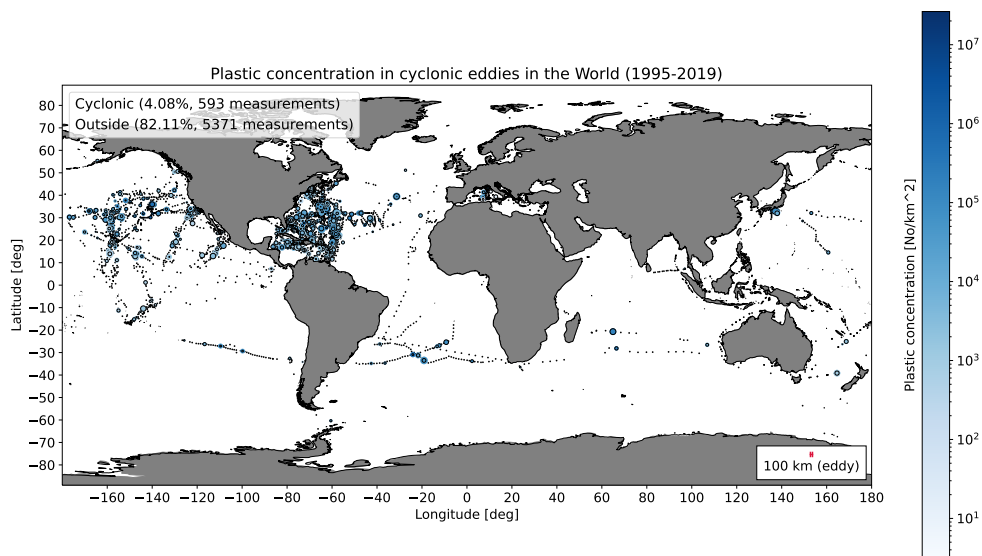
(a) North Atlantic region

(b) North Pacific region

Figure A.1: Plastic concentration with radius representing chlorophyll concentration in the areas of interest
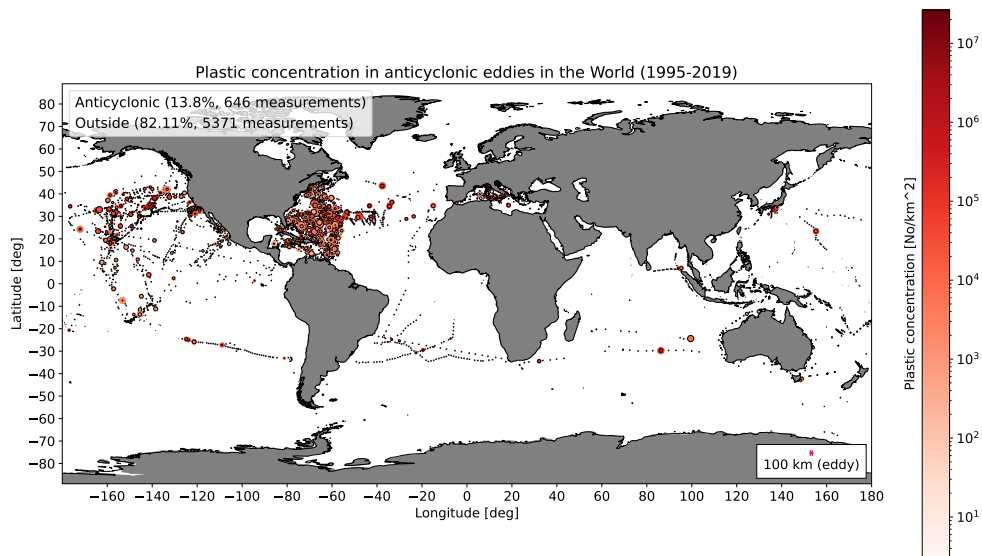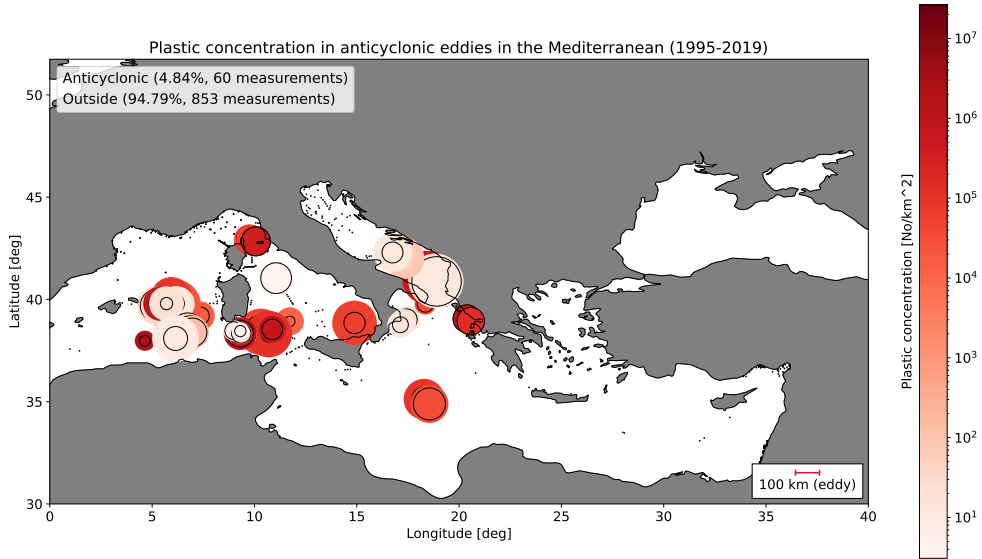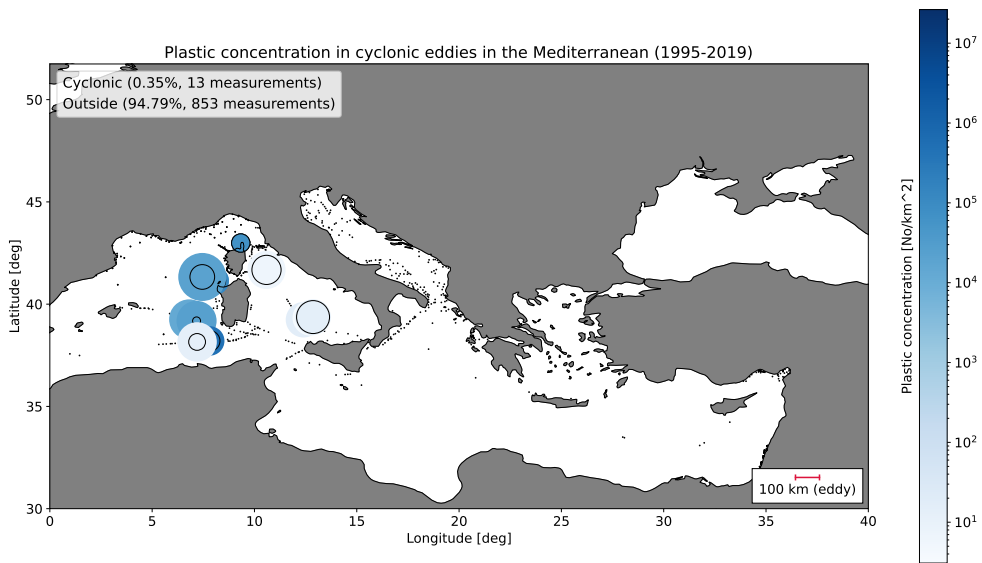
(a) Anticyclonic case

(b) Cyclonic case

Figure A.2: Plastic concentration in anticyclonic/cyclonic eddies in the global ocean

(a) Anticyclonic case

(b) Cyclonic case

Figure A.3: Plastic concentration in anticyclonic/cyclonic eddies in the Mediterranean